Pro(−) and Pro(+) samples for each subject, and the quantity difference was also obtained by subtracting the 16S read number of the Pro(+) samples from that of the Pro(−) samples. This is because OTUs showing a high quantity difference, but less fold change may also have substantial influence on gut microbiota composition. We found several OTUs significantly changed by probiotic administration, including OTUs assigned to both the indigenous and administrated strains (Fig. 5). We listed 88 OTUs (7.5% of all analysed 1175 OTUs) showing significant change of ≥3-fold, among which 30 OTUs changed by ≥10-fold (Supplementary Fig. S5). We excluded 6 OTUs assigned to the administrated strains from the 30 OTUs and obtained 24 OTUs assigned to the indigenous species, including OTU00072 assigned to *Streptococcus salivarius* that showed significant change in 2 subjects (Supplementary Table S9). We also found seven OTUs showing significant difference in quantity between both samples (Supplementary Table S10). Of the combined 32 OTUs (2.7%), 18 were increased and 14 were decreased by probiotic administration. Many of the OTUs showing a significant increase were assigned to minority species in the Pro(−) samples, but some increased up to nearly 7% in abundance (e.g. OTU00372 assigned to *Eubacterium rectale*). On the other hand, the OTUs showing a significant decrease were almost undetected in the Pro(+) samples. Phylum-level species assignment showed that species belonging to the phylum *Firmicutes* were most largely affected by both probiotics, and all species belonging to the phylum *Bacteroidetes* were affected only by *Lactobacillus* probiotics (Table 1). The 32 OTUs were assigned to 27 indigenous species, among which 4 species (*Clostridium clostridioforme*, *Eubacterium eligens*, *E. rectale*, and *Faecalibacterium prausnitzii*) were assigned by 8 different OTUs and 1 species (*S. salivarius*) was assigned by the 2 same OTUs as described above. All these species except for *S. salivarius* were found to show significant change only in one subject, indicating that response of the indigenous species to probiotics is highly individual specific (Supplementary Fig. S6). Two different OTUs (OTU02677 and OTU02748) assigned to *F. prausnitzii*, of which the reduction is known to be correlated with inflammatory bowel disease,[70] were found to both decrease and increase in the same subject (APr40) by probiotic administration, suggesting that these two phylogenetically close species may have the diversity of response to probiotic action. We also examined distribution of the 32 OTUs in the subjects. The results revealed that 4 subjects

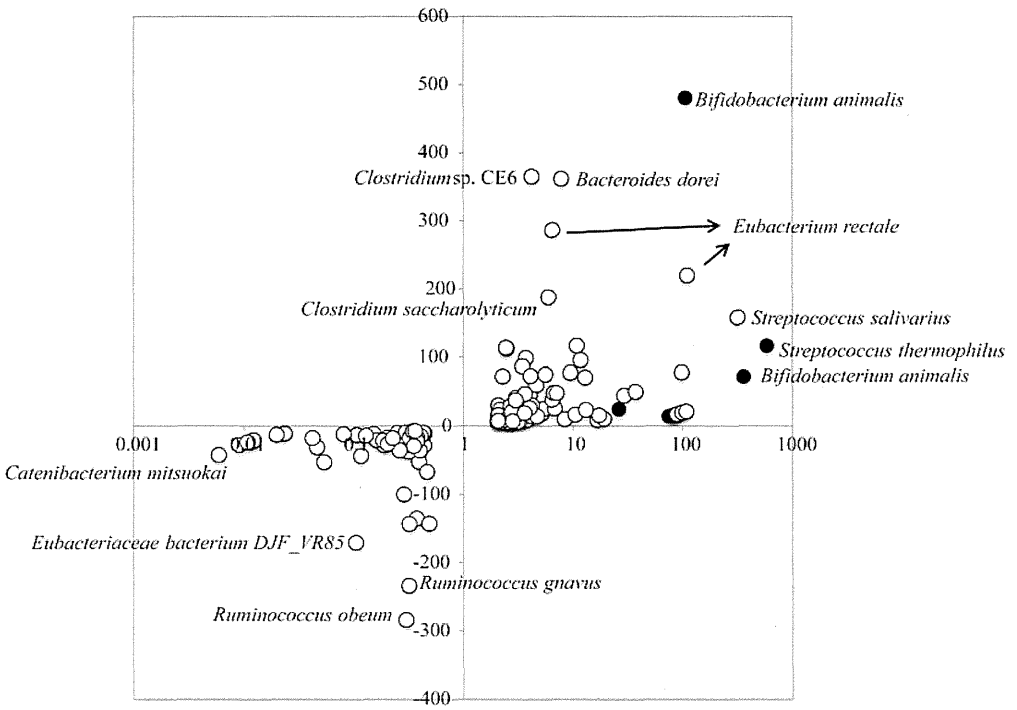


**Figure 5.** OTUs showing ≥2-fold change and their difference in quantity between the Pro(−) and Pro(+) samples. The *x*-axis represents the scale of fold change between the Pro(+) and Pro(−) samples. The *y*-axis represents the difference (number of reads) in quantity between the Pro(+) and Pro(−) samples. Closed and open circles indicate the administrated probiotic and indigenous species, respectively.

**Table 1.** Phylum-level species assignment of OTUs showing significant fold change or quantity difference by administration of probiotics

| Type of probiotics | Change | [a]Number of varied OTUs | Fold change (≥10-fold) | | | | Number of varied OTUs | Difference (≥150 reads) | |
|---|---|---|---|---|---|---|---|---|---|
| | | | Firmicutes | Actinobacteria | Bacteroidetes | Unclassified bacterium | | Firmicutes | Bacteroidetes |
| Lactobacillus | Increase | 9 | 7 | 0 | 1 | 1 | 3 | 2 | 1 |
| | Decrease | 7 | 3 | 1 | 3 | 0 | 1 | 1 | 0 |
| | Total | 16 | 10 | 1 | 4 | 1 | 4 | 3 | 1 |
| Bifidobacterium | Increase | 5 | 5 | 0 | 0 | 0 | 1 | 1 | 0 |
| | Decrease | 4 | 4 | 0 | 0 | 0 | 2 | 2 | 0 |
| | Total | 9 | 9 | 0 | 0 | 0 | 3 | 3 | 0 |
| All | Increase | 14 | 12 | 0 | 1 | 1 | 4 | 3 | 1 |
| | Decrease | 11 | 7 | 1 | 3 | 0 | 3 | 3 | 0 |
| | Total | 25 | 19 | 1 | 4 | 1 | 7 | 6 | 1 |

[a]Administrated probiotic strains were excluded, and only OTUs with a $P$-value $< 0.05$ are shown.

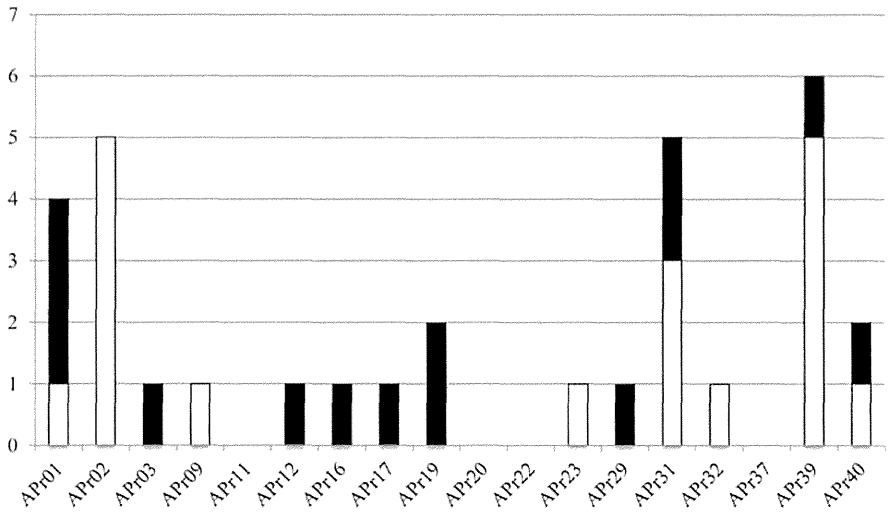


**Figure 6.** Distribution of 32 OTUs showing a significant change in 18 subjects. The $y$-axis indicates the number of OTUs showing significant change between the Pro(−) and Pro(+) samples in each subject (see Supplementary Tables S9 and S10). Open and closed bars indicate increased and decreased OTUs, respectively.

(APr11, 20, 22, and 37) did not have such OTUs and 8 subjects had only 1 OTU, whereas 4 subjects (APr01, 02, 31, and 39) had more than 4 OTUs showing significant change (Fig. 6), suggesting their uneven distribution in the 18 subjects. These data imply existence of the sensitive and less sensitive responders to probiotic action and if so, it would be interesting to investigate the relation between gut microbiota type and its response to probiotics.

In summary, we analysed changes of the gut microbiota composition of healthy adults fed with probiotics using the 454 pyrosequencing platform with the improved quantitative accuracy for evaluation of the overall bacterial composition. The present study using large datasets enabled us to more comprehensively and precisely evaluate the effect of probiotics on gut microbiota than the previous probiotic intervention researches in which the analysis exclusively focussed on only several limited bacterial species using conventional methods. Our data further support the high inter-subject variability and the high intra-subject stability that is the current common view for the feature of adult gut microbiota. A recent study of gut microbiota in twins demonstrated that probiotics had almost no effect on the community structure, but affected the gene expression of microbiota.[39] To more deeply understand the potential function of probiotics, the analysis of bacterial and host cell's transcriptome and intestinal metabolome is required.

**Acknowledgements:** We thank Dr Todd D. Taylor for critical reading of the manuscript, and K. Furuya, C. Shindo, H. Inaba, E. Iioka, Y. Takayama, E. Ohmori, M. Kiuchi, Y. Hattori (The University of Tokyo), and A. Nakano (Azabu University) for technical support.

**Supplementary data:** Supplementary Data are available at www.dnaresearch.oxfordjournals.org.

## Funding

This work was supported in part by the global COE project of 'Genome Information Big Bang' from the Ministry of Education, Culture, Sports, Science, and Technology (MEXT) of Japan (to M.H. and K.O.), a research project grant from Azabu University to H.M. and by a grant from the Core Research for Evolutional Science and Technology (CREST) program of the Japan Science and Technology Agency (JST) to K.O.

## References

1. Preidis, G.A. and Versalovic, J. 2009, Targeting the human microbiome with antibiotics, probiotics, and prebiotics: gastroenterology enters the metagenomics era, *Gastroenterology*, **136**, 2015–31.
2. Patel, R.M. and Lin, P.W. 2010, Developmental biology of gut-probiotic interaction, *Gut Microbes*, **1**, 186–95.
3. Gerritsen, J., Smidt, H., Rijkers, G.T. and de Vos, W.M. 2011, Intestinal microbiota in human health and disease: the impact of probiotics, *Genes Nutr.*, **6**, 209–40.
4. Sanders, M.E., Heimbach, J.T., Pot, B., et al. 2011, Health claims substantiation for probiotic and prebiotic products, *Gut Microbes*, **2**, 127–33.
5. Aureli, P., Capurso, L., Castellazzi, A.M., et al. 2011, Probiotics and health: an evidence-based review, *Pharmacol. Res.*, **63**, 366–76.
6. Rauch, M. and Lynch, S.V. 2012, The potential for probiotic manipulation of the gastrointestinal microbiome, *Curr. Opin. Biotechnol.*, **23**, 192–201.
7. Fujimura, K.E., Slusher, N.A., Cabana, M.D. and Lynch, S.V. 2010, Role of the gut microbiota in defining human health, *Expert Rev. Anti Infect. Ther.*, **8**, 435–54.
8. Deshpande, G.C., Rao, S.C., Keil, A.D. and Patole, S.K. 2011, Evidence-based guidelines for use of probiotics in preterm neonates, *BMC Med.*, **9**, 92.
9. Bron, P.A., van Baarlen, P. and Kleerebezem, M. 2011, Emerging molecular insights into the interaction between probiotics and the host intestinal mucosa, *Nat. Rev. Microbiol.*, **10**, 66–78.
10. Thomas, D.W., Greer, F.R., American Academy of Pediatrics Committee on Nutrition; American Academy of Pediatrics Section on Gastroenterology, Hepatology, and Nutrition. 2010, Probiotics and prebiotics in pediatrics, *Pediatrics*, **126**, 1217–31.
11. Indrio, F. and Neu, J.N. 2011, The intestinal microbiome of infants and the use of probiotics, *Curr. Opin. Pediatr.*, **23**, 145–50.
12. Saxelin, M., Tynkkynen, S., Mattila-Sandholm, T. and de Vos, W.M. 2005, Probiotic and other functional microbes: from markets to mechanisms, *Curr. Opin. Biotechnol.*, **16**, 204–11.
13. Nagpal, R., Kumar, A., Kumar, M., Behare, P.V., Jain, S. and Yadav, H. 2012, Probiotics, their health benefits and applications for developing healthier foods: a review, *FEMS Microbiol. Lett.*, **334**, 1–15.
14. Bisanz, J.E. and Reid, G. 2011, Unraveling how probiotic yogurt works, *Sci. Transl. Med.*, **3**, 106ps41.
15. Bron, P.A. and Kleerebezem, M. 2011, Engineering lactic acid bacteria for increased industrial functionality, *Bioeng. Bugs*, **2**, 80–7.
16. Kleerebezem, M. and Vaughan, E.E. 2009, Probiotic and gut lactobacilli and bifidobacteria: molecular approaches to study diversity and activity, *Annu. Rev. Microbiol.*, **63**, 269–90.
17. Ventura, M., O'Flaherty, S., Claesson, M.J., et al. 2009, Genome-scale analyses of health-promoting bacteria: probiogenomics, *Nat. Rev. Microbiol.*, **7**, 61–71.
18. Snydman, D.R. 2008, The safety of probiotics, *Clin. Infect. Dis.*, **46**, S104–11.
19. Lozupone, C.A., Stombaugh, J.I., Gordon, J.I., Jansson, J.K. and Knight, R. 2012, Diversity, stability and resilience of the human gut microbiota, *Nature*, **489**, 220–30.
20. Clemente, J.C., Ursell, L.K., Parfrey, L.W. and Knight, R. 2012, The impact of the gut microbiota on human health: an integrative view, *Cell*, **148**, 1258–70.
21. Nicholson, J.K., Holmes, E., Kinross, J., et al. 2012, Host-gut microbiota metabolic interactions, *Science*, **336**, 1262–7.
22. Walter, J. and Ley, R. 2011, The human gut microbiome: ecology and recent evolutionary changes, *Annu. Rev. Microbiol.*, **65**, 411–29.
23. Hooper, L.V., Littman, D.R. and Macpherson, A.J. 2012, Interactions between the microbiota and the immune system, *Science*, **336**, 1268–73.
24. Tannock, G.W., Munro, K., Harmsen, H.J., Welling, G.W., Smart, J. and Gopal, P.K. 2000, Analysis of the fecal microflora of human subjects consuming a probiotic product containing *Lactobacillus rhamnosus* DR20, *Appl. Environ. Microbiol.*, **66**, 2578–88.
25. García-Albiach, R., Pozuelo de Felipe, M.J., Angulo, S., et al. 2008, Molecular analysis of yogurt containing *Lactobacillus delbrueckii* subsp. bulgaricus and *Streptococcus thermophilus* in human intestinal microbiota, *Am. J. Clin. Nutr.*, **87**, 91–6.
26. Alvaro, E., Andrieux, C., Rochet, V., et al. 2007, Composition and metabolism of the intestinal microbiota in consumers and non-consumers of yogurt, *Br. J. Nutr.*, **97**, 126–33.
27. Rochet, V., Rigottier-Gois, L., Levenez, F., et al. 2008, Modulation of *Lactobacillus casei* in ileal and fecal samples from healthy volunteers after consumption of a fermented milk containing *Lactobacillus casei* DN-114 001Rif, *Can. J. Microbiol.*, **54**, 660–7.
28. Rochet, V., Rigottier-Gois, L., Ledaire, A., et al. 2008, Survival of *Bifidobacterium animalis* DN-173 010 in the faecal microbiota after administration in lyophilized form or in fermented product – a randomised study in healthy adults, *J. Mol. Microbiol. Biotechnol.*, **14**, 128–36.
29. Ouwehand, A.C., Bergsma, N., Parhiala, R., et al. 2008, Bifidobacterium microbiota and parameters of immune function in elderly subjects, *FEMS Immunol. Med. Microbiol.*, **53**, 18–25.

30. Firmesse, O., Mogenet, A., Bresson, J.L., Corthier, G. and Furet, J.P. 2008, *Lactobacillus rhamnosus* R11 consumed in a food supplement survived human digestive transit without modifying microbiota equilibrium as assessed by real-time polymerase chain reaction, *J. Mol. Microbiol. Biotechnol.*, **14**, 90–9.
31. Lahtinen, S.J., Tammela, L., Korpela, J., et al. 2009, Probiotics modulate the Bifidobacterium microbiota of elderly nursing home residents, *Age (Dordr)*, **31**, 59–66.
32. Savard, P., Lamarche, B., Paradis, M.E., Thiboutot, H., Laurin, É. and Roy, D. 2011, Impact of *Bifidobacterium animalis* subsp. lactis BB-12 and, *Lactobacillus acidophilus* LA-5-containing yoghurt, on fecal bacterial counts of healthy adults, *Int. J. Food Microbiol.*, **149**, 50–7.
33. Yamano, T., Iino, H., Takada, M., Blum, S., Rochat, F. and Fukushima, Y. 2006, Improvement of the human intestinal flora by ingestion of the probiotic strain *Lactobacillus johnsonii* La1, *Br. J. Nutr.*, **95**, 303–12.
34. Engelbrektson, A.L., Korzenik, J.R. and Sanders, M.E. 2006, Analysis of treatment effects on the microbial ecology of the human intestine, *FEMS Microbiol. Ecol.*, **57**, 239–50.
35. Marzotto, M., Maffeis, C., Paternoster, T., et al. 2006, *Lactobacillus paracasei* A survives gastrointestinal passage and affects the fecal microbiota of healthy infants, *Res. Microbiol.*, **157**, 857–66.
36. Cox, M.J., Huang, Y.J., Fujimura, K.E., et al. 2010, *Lactobacillus casei* abundance is associated with profound shifts in the infant gut microbiome, *PLoS One*, **5**, e8745.
37. Culligan, E.P., Hill, C. and Sleator, R.D. 2009, Probiotics and gastrointestinal disease: successes, problems and future prospects, *Gut Pathog.*, **1**, 19.
38. Gareau, M.G., Sherman, P.M. and Walker, W.A. 2010, Probiotics and the gut microbiota in intestinal health and disease, *Nat. Rev. Gastroenterol. Hepatol.*, **7**, 503–14.
39. McNulty, N.P., Yatsunenko, T., Hsiao, A., et al. 2011, The impact of a consortium of fermented milk strains on the gut microbiome of gnotobiotic mice and monozygotic twins, *Sci. Transl. Med.*, **3**, 106ra106.
40. Metzker, M.L. 2010, Sequencing technologies—the next generation, *Nat. Rev. Genet.*, **11**, 31–46.
41. Qin, J., Li, R., Raes, J., et al. 2010, A human gut microbial gene catalogue established by metagenomic sequencing, *Nature*, **464**, 59–65.
42. Huse, S.M., Dethlefsen, L., Huber, J.A., Mark, WD., Relman, D.A. and Sogin, M.L. 2008, Exploring microbial diversity and taxonomy using SSU rRNA hypervariable tag sequencing, *PLoS Genet.*, **4**, e1000255.
43. Huse, S.M., Huber, J.A., Morrison, H.G., Sogin, M.L. and Welch, D.M. 2007, Accuracy and quality of massively parallel DNA pyrosequencing, *Genome Biol.*, **8**, R143.
44. Hamady, M., Lozupone, C. and Knight, R. 2010, Fast Unifrac: facilitating high-throughput phylogenetic analysis of microbial communities including analysis of pyrosequencing and PhyloChip data, *ISME J.*, **4**, 17–27.
45. Droege, M. and Hill, B. 2008, The Genome Sequencer FLX System—longer reads, more applications, straight forward bioinformatics and more complete data sets, *J. Biotechnol.*, **136**, 3–10.
46. Andersson, A.F., Lindberg, M., Jakobsson, H., Bäckhed, F., Nyrén, P. and Engstrand, L. 2008, Comparative analysis of human gut microbiota by barcoded pyrosequencing, *PLoS One*, **3**, e2836.
47. Kuczynski, J., Lauber, C.L., Walters, W.A., et al. 2011, Experimental and analytical tools for studying the human microbiome, *Nat. Rev. Genet.*, **13**, 47–58.
48. Hamady, M., Walker, J.J., Harris, J.K., Gold, N.J. and Knight, R. 2008, Error-correcting barcoded primers for pyrosequencing hundreds of samples in multiplex, *Nat. Methods*, **5**, 235–7.
49. Morita, H., Kuwahara, T., Ohshima, K., et al. 2007, An improved isolation method for metagenomic analysis of the microbial flora of the human intestine, *Microbes Environ.*, **22**, 214–22.
50. Claesson, M.J., Wang, Q., O'Sullivan, O., et al. 2010, Comparison of two next-generation sequencing technologies for resolving highly complex microbiota composition using tandem variable 16S rRNA gene regions, *Nucleic Acids Res.*, **38**, e200.
51. Zhou, H.W., Li, D.F., Tam, N.F., et al. 2011, BIPES, a cost-effective high-throughput method for assessing microbial diversity, *ISME J.*, **5**, 741–9.
52. Hattori, M. and Taylor, T.D. 2009, The human intestinal microbiome: a new frontier of human biology, *DNA Res.*, **16**, 1–12.
53. Frank, J.A., Reich, C.I., Sharma, S., Weisbaum, J.S., Wilson, B.A. and Olsen, G.J. 2008, Critical evaluation of two primers commonly used for amplification of bacterial 16S rRNA genes, *Appl. Environ. Microbiol.*, **74**, 2461–70.
54. Hill, J.E., Fernando, W.M., Zello, G.A., Tyler, R.T., Dahl, W.J. and Van Kessel, A.G. 2010, Improvement of the representation of bifidobacteria in fecal microbiota metagenomic libraries by application of the cpn60 universal primer cocktail, *Appl. Environ. Microbiol.*, **76**, 4550–2.
55. Palmer, C. 2007, Development of the human infant intestinal microbiota, *PLoS Biol.*, **5**, 1556–73.
56. Haas, B.J., Gevers, D., Earl, A.M., et al. 2011, Chimeric 16S rRNA sequence formation and detection in Sanger and 454-pyrosequenced PCR amplicons, *Genome Res.*, **21**, 494–504.
57. Schloss, P.D., Gevers, D. and Westcott, S.L. 2011, Reducing the effects of PCR amplification and sequencing artifacts on 16S rRNA-based studies, *PLoS One*, **6**, e27310.
58. Gilles, A., Meglécz, E., Pech, N., Ferreira, S., Malausa, T. and Martin, J.F. 2011, Accuracy and quality assessment of 454 GS-FLX Titanium pyrosequencing, *BMC Genomics*, **12**, 245.
59. Quince, C., Lanzén, A., Curtis, T.P., et al. 2009, Accurate determination of microbial diversity from 454 pyrosequencing data, *Nat. Methods*, **6**, 639–41.
60. Diaz, P.I., Dupuy, A.K., Abusleme, L., et al. 2012, Using high throughput sequencing to explore the biodiversity in oral bacterial communities, *Mol. Oral Microbiol.*, **27**, 182–201.
61. Schloss, P.D. and Handelsman, J. 2005, Introducing DOTUR, a computer program for defining operational

taxonomic units and estimating species richness, *Appl. Environ. Microbiol.*, **71**, 1501–6.
62. del Campo, R., Bravo, D., Cantón, R., et al. 2005, Scarce evidence of yogurt lactic acid bacteria in human feces after daily yogurt consumption by healthy volunteers, *Appl. Environ. Microbiol.*, **71**, 547–9.
63. Oozeer, R., Leplingard, A., Mater, D.D., et al. 2006, Survival of *Lactobacillus casei* in the human digestive tract after consumption of fermented milk, *Appl. Environ. Microbiol.*, **72**, 5615–7.
64. Marco, M.L., de Vries, M.C., Wels, M., et al. 2010, Convergence in probiotic Lactobacillus gut-adaptive responses in humans and mice, *ISME J.*, **4**, 1481–4.
65. Manichanh, C., Rigottier-Gois, L., Bonnaud, E., et al. 2006, Reduced diversity of fecal microbiota in Crohn's disease revealed by a metagenomic approach, *Gut*, **55**, 205–11.
66. Turnbaugh, P.J., Hamady, M.H., Yatsuneko, T., et al. 2009, A core gut microbiome in obese and lean twins, *Nature*, **475**, 480–4.
67. Kurokawa, K., Itoh, T., Kuwahara, T., et al. 2007, Comparative metagenomics revealed commonly enriched gene sets in human gut microbiomes, *DNA Res.*, **14**, 169–81.
68. Jernberg, C., Löfmark, S., Edlund, C. and Jansson, J.K. 2007, Long-term ecological impacts of antibiotic administration on the human intestinal microbiota, *ISME J.*, **1**, 56–66.
69. Wu, G.D., Chen, J., Hoffmann, C., et al. 2011, Linking long-term dietary patterns with gut microbial enterotypes, *Science*, **334**, 105–8.
70. Sokol, H., Seksik, P., Furet, J.P., et al. 2009, Low counts of *Faecalibacterium prausnitzii* in colitis microbiota, *Inflamm. Bowel Dis.*, **15**, 1183–9.

Multiple Sclerosis and Related Disorders (2014) 3, 94-106

Available online at www.sciencedirect.com

ScienceDirect

journal homepage: www.elsevier.com/locate/msard

# Molecular network of ChIP-Seq-based NF-κB p65 target genes involves diverse immune functions relevant to the immunopathogenesis of multiple sclerosis

**Jun-ichi Satoh***

*Department of Bioinformatics and Molecular Neuropathology, Meiji Pharmaceutical University, 2-522-1 Noshio, Kiyose, Tokyo 204-8588, Japan*

Received 18 December 2012; received in revised form 24 April 2013; accepted 30 April 2013

**KEYWORDS**
ChIP-Seq;
GenomeJack;
Molecular network;
Multiple sclerosis;
Next generation sequencing;
NF-κB

**Abstract**
*Background:* The transcription factor nuclear factor-kappa B (NF-κB) acts as a central regulator of immune response, stress response, cell proliferation, and apoptosis. Aberrant regulation of NF-κB function triggers development of cancers, metabolic diseases, and autoimmune diseases. We attempted to characterize a global picture of the NF-κB target gene network relevant to the immunopathogenesis of multiple sclerosis (MS).
*Methods:* We identified the comprehensive set of 918 NF-κB p65 binding sites on protein-coding genes from chromatin immunoprecipitation followed by deep sequencing (ChIP-Seq) dataset of TNFα-stimulated human B lymphoblastoid cells. The molecular network was studied by a battery of pathway analysis tools of bioinformatics.
*Results:* The GenomeJack genome viewer showed that NF-κB p65 binding sites were accumulated in promoter (35.5%) and intronic (54.9%) regions with an existence of the NF-κB consensus sequence motif. A set of 52 genes (5.7%) corresponded to known NF-κB targets by database search. KEGG, PANTHER, and Ingenuity Pathways Analysis (IPA) revealed that the NF-κB p65 target gene network is linked to regulation of immune functions and oncogenesis, including B cell receptor signaling, T cell activation pathway, Toll-like receptor signaling, and apoptosis signaling, and molecular mechanisms of cancers. KeyMolnet indicated an involvement of the complex crosstalk among core transcription factors in the NF-κB p65 target gene network. Furthermore, the set of NF-κB p65 target genes included 10 genes among 98 MS risk alleles and 49 molecules among 709 MS brain lesion-specific proteins.
*Conclusions:* These results suggest that aberrant regulation of NF-κB-mediated gene expression, by inducing dysfunction of diverse immune functions, is closely associated with development and progression of MS.


*Tel./fax: +81 42 495 8678.
*E-mail address:* satoj@my-pharm.ac.jp

2211-0348/$ - see front matter © 2013 Elsevier B.V. All rights reserved.
http://dx.doi.org/10.1016/j.msard.2013.04.005

## 1. Introduction

The transcription factor nuclear factor-kappa B (NF-κB) acts as a central regulator of innate and adaptive immune response, stress response, cell proliferation, and apoptosis (Barnes and Karin, 1997; Hayden et al., 2006). Deregulation of NF-κB function triggers development of cancers, metabolic diseases, and autoimmune diseases, such as multiple sclerosis (MS) and rheumatoid arthritis (RA) (Yan and Greer, 2008; Gregersen et al., 2009). The NF-κB family proteins consist of five members, such as RelA (p65), RelB, c-Rel, NF-κB1 (p105), and NF-κB2 (p100) (Gilmore, 2006). The latter two are proteolytically processed into p50 and p52, respectively. All the members share the Rel homology domain (RHD) acting for DNA binding and dimerization. The NF-κB family proteins constitute either homodimers or heterodimers, except for RelB that exclusively forms heterodimers. The p50-RelA heterodimer represents a predominant NF-κB dimer in various cell types. The NF-κB dimers interact with specific DNA sequences named the κB site located on promoters to activate or repress transcription of target genes. Only p65 and c-Rel act as a potent transcriptional activator, whereas p50 and p52 homodimers generally repress transcription (Rothwarf and Karin, 1999). Optimal induction of NF-κB target genes requires phosphorylation of p65 within its transactivation domain in response to distinct stimuli by various kinases (Viatour et al., 2005).

NF-κB activity is regulated tightly at multiple levels (Viatour et al., 2005; Gilmore, 2006). In unstimulated cells, NF-κB proteins exist in an inactive state, being sequestrated in the cytoplasm via non-covalent interaction with the inhibitor of NF-κB (IκB) proteins, such as IκBα, IκBβ, IκBγ, and IκBε. Viral and bacterial products, cytokines, and oxidative stress activate the specific IκB kinase (IKK) complex, composed of two catalytic kinase subunits called IKKα and IKKβ and a regulatory subunit called NF-κB essential modulator (NEMO). IκB proteins, when phosphorylated by the IKK complex, are ubiquitinated, and processed for 26 S proteasome-mediated degradation, resulting in nuclear translocation of NF-κB dimers. The NF-κB signaling cascade is categorized into canonical and non-canonical pathways (Oeckinghaus et al., 2011). The canonical pathway is activated by various proinflammatory cytokines, such as tumor necrosis factor-alpha tumor necrosis factor-alpha (TNFα) and interleukin-1 (IL-1), transduced by both IKKβ and NEMO that chiefly mediate phosphorylation of IκBα, followed by nuclear translocation of p65-containing NF-κB heterodimers. The non-canonical pathway, activated by CD40 ligand, B-cell activating factor (BAFF), and lymphotoxin-beta (LTβ), requires IKKα-mediated phosphorylation of p100 dimerized with RelB, which are processed to form the p52-RelB complex.

MS is an inflammatory demyelinating disease of the central nervous system (CNS) white matter, presenting with a relapsing-remitting (RR) and/or progressive clinical course. It is mediated by an autoimmune process triggered by a complex interplay between genetic and environmental factors, leading to development of autoreactive T helper type 1 (Th1) and type 17 (Th17) lymphocytes (Comabella and Khoury, 2012). Several lines of evidence indicate that aberrant regulation of NF-κB signaling pathway plays a central role in acute relapse of MS. By gene expression profiling, we identified 43 differentially expressed genes in peripheral blood $CD3^+$ T cells between the peak of acute relapse and the complete remission of RRMS (Satoh et al., 2008). We found that the molecular network of 43 genes showed the most significant relationship with transcriptional regulation by NF-κB. Our observations are supported by several studies that verified an aberrant expression of NF-κB signaling molecules in peripheral blood mononuclear cells (PMBC) during MS relapse (Achiron et al., 2007; Lindsey et al., 2011). Intravenous methylprednisolone pulse (IVMP) immediately reduces the levels of activated p65 in PBMC of MS patients (Eggert et al., 2008). Furthermore, interferon-gamma (IFNγ, a prototype Th1 cytokine, is identified as one of NF-κB target genes (Sica et al., 1997), while interferon-beta (IFNβ, the first-line medication for RRMS, attenuates proinflammatory responses by inhibiting the NF-κB activity in lymphocytes (Martín-Saavedra et al., 2007). Mucosa-associated lymphoid tissue lymphoma translocation gene 1 (MALT1), a key regulator of NF-κB activation, positively regulates the encephalitogenic potential of inflammatory Th17 cells (Brüstle et al., 2012). To elucidate the precise role of NF-κB in MS relapse, it is highly important to thoroughly characterize NF-κB target genes involved in the immunopathogenesis of MS.

A number of previous studies identified hundreds of NF-κB target genes, including those involved in not only inflammatory and anti-apoptotic responses, but also anti-inflammatory and proapoptotic responses (Pahl, 1999). Importantly, NF-κB target genes often activate NF-κB itself, providing a positive regulatory loop that amplifies and perpetuates inflammatory responses (Barnes and Karin, 1997). However, it remains unclear how many of previously identified genes actually represent direct targets for NF-κB-mediated transcriptional activation.

Recently, the rapid progress in the next-generation sequencing (NGS) technology has revolutionized the field of genome research. As one of NGS applications, chromatin immunoprecipitation followed by deep sequencing (ChIP-Seq) provides a highly efficient method for genome-wide profiling of DNA-binding proteins, histone modifications, and nucleosomes (Park, 2009). ChIP-Seq endowed with an advantage of higher resolution, less noise, and greater coverage of the genome, compared with the microarray-based ChIP-Chip method, serves as an innovative tool for studying the comprehensive gene regulatory networks. However, since the NGS analysis produces extremely high-throughput experimental data, it is often difficult to extract the meaningful biological implications. Recent advances in systems biology enable us to illustrate the cell-wide map of the complex molecular interactions by using the literature-based knowledgebase of molecular pathways (Satoh, 2010). The logically arranged molecular networks construct the whole system characterized by robustness, which maintains the proper function of the system in the face of genetic and environmental perturbations. Therefore, the integration of high dimensional NGS data with underlying molecular networks offers a rational approach to characterize the network-based molecular mechanisms of gene regulation on the whole genome scale.

In the present study, to characterize a global picture of the NF-κB target gene network, we investigated the NF-κB p65 ChIP-Seq dataset of TNFα-stimulated human B lymphoblastoid cells. The dataset was retrieved from the public

database of the Encyclopedia of DNA Elements (ENCODE) project (encodeproject.org/ENCODE) (Kasowski et al., 2010; Gerstein et al., 2012).

## 2. Methods

### 2.1. ChIP-Seq dataset

To identify a comprehensive set of NF-κB p65-target genes, we studied a series of ChIP-Seq data retrieved from DDBJ Sequence Read Archive (DRA) under the accession number of SRP007993. The ChIP-Seq experiments were performed for the ENCODE project by researchers in Dr. Michel Snyder's Laboratory, Stanford University (Kasowski et al., 2010). The data were derived from 10 distinct Epstein-Barr virus (EBV)-transformed human lymphoblastoid cell lines (LCL) numbered GM10847, GM12878, GM12891, GM12892, GM15510, GM18505, GM18526, GM18951, GM19099, and GM19193. In these experiments, the cells were exposed for 6 h to 25 ng/mL recombinant human TNFα (#14-8329-62; eBioscience), and then were fixed with formaldehyde to crosslink NF-κB-DNA complexes, and immunoprecipitated from sonicated nuclear lysates by using rabbit anti-NF-κB p65 antibody (sc-372; Santa Cruz Biotechnology) or normal rabbit IgG for input control. NGS libraries were constructed from 120 to 350 bp size-selected ChIP DNA fragments. They were processed for deep sequencing at a 28 bp read length on Genome Analyzer II (Illumina).

We converted SRALite-formatted files into FASTQ-formatted files, and combined 10 antibody-treated samples into the "test set" and 10 corresponding input controls into the "control set". We mapped these data on the human genome reference sequence hg19 by using the Bowtie 0.12.7 program (bowtie-bio.sourceforge.net). Subsequently, we identified statistically significant peaks of mapped reads by using the MACS program (liulab.dfci.harvard.edu/MACS) under the stringent condition that satisfies the false discovery rate (FDR) ≤0.1% and fold enrichment ≥10 to avoid the detection of false positive binding sites if at all possible. Then, we identified the genomic location of MACS peaks by importing the processed data into GenomeJack v1.4, a novel genome viewer for NGS platforms developed by Mitsubishi Space Software (www.mss.co.jp/businessfield/bioinformatics). Based on RefSeq ID, MACS peaks were categorized into the following; the peaks located on protein-coding genes supplemented with NM-heading

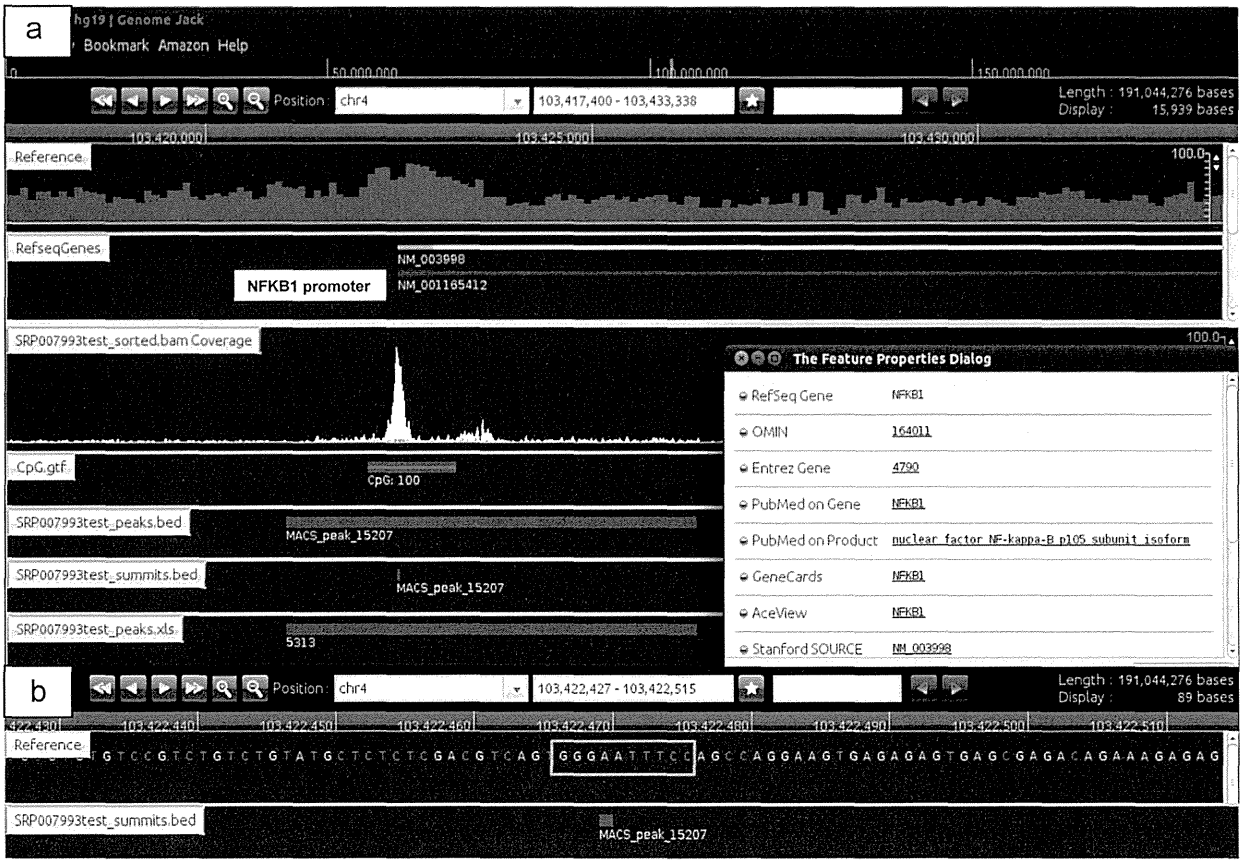


**Fig. 1** Location of NF-κB p65 ChIP-Seq peaks in the promoter region of target genes. From the dataset numbered SRP007993, we identified totally 1630 stringent ChIP-Seq peaks that satisfied the criteria of both FDR ≤ 0.1% and fold enrichment ≥ 10. The genomic location of the peaks was determined by importing the processed data into GenomeJack. An example of NF-κB p105 subunit (NFKB1) (Entrez Gene ID 4790 in Table 1), composed of two transcript variants NM_003998 and NM_001165412, is shown, where a MACS peak numbered 15207 is located in the promoter region of NFKB1 (panel a) with a NF-κB consensus sequence motif highlighted by an orange square (panel b). (For interpretation of the references to color in this figure legend, the reader is referred to the web version of this article.)

numbers, the peaks located on non-coding genes supplemented with NR-heading numbers, and the peaks located in intergenic regions with no relevant neighboring genes. Genomic locations of the peaks were further classified into the following; the promoter region defined by the location within a 5 kb upstream from the 5′ end of genes, the 5′ untranslated region (5′UTR), the exon, the intron, the 3′ UTR, and intergenic regions outside these, as described previously (Satoh and Tabunoki, in press).

The consensus sequence motif was identified by importing a 400 bp-length sequence surrounding the summit of MACS peaks into the MEME-ChIP program (meme.sdsc.edu/meme/cgi-bin/meme-chip.cgi). The information on known NF-κB target genes was collected from web accessible databases constructed by Dr. Thomas Gilmore, Boston University (www.bu.edu/nf-kb/gene-resources/target-genes) and by Bonsai Bioinformatics, the Laboratoire d'Informatique Fondamentale de Lille (LIFL), Université Lille 1 (bioinfo.lifl.fr/NF-KB).

## 3. Molecular network analysis

To identify biologically relevant molecular networks and pathways, we imported Entrez Gene IDs of NF-κB p65 target genes into the Functional Annotation tool of Database for Annotation, Visualization and Integrated Discovery (DAVID) v6.7 (david.abcc.ncifcrf.gov) (Huang et al., 2009). DAVID identifies relevant pathways constructed by Kyoto Encyclopedia of Genes and Genomes (KEGG) (www.kegg.jp) or by the Protein Analysis Through Evolutionary Relationships (PANTHER) classification system (www.pantherdb.org). They are comprised of the genes enriched in the given set with statistical significance evaluated by the modified Fisher's exact test corrected by Bonferroni's multiple comparison test. KEGG is a publicly accessible knowledgebase containing manually curated reference pathways that cover a wide range of metabolic, genetic, environmental, and cellular processes, and human diseases, currently composed of 207,161 pathways generated from 432 reference pathways. PANTHER includes the information on 175 signaling and metabolic pathways manually curated by expert biologists, expressed in a Systems Biology Markup Language (SBML) format. We also imported Entrez Gene IDs into Ingenuity Pathways Analysis (IPA) (Ingenuity Systems; www.ingenuity.com) and KeyMolnet (Institute of Medicinal Molecular Design; www.immd.co.jp), both of which are commercial tools for molecular network analysis.

IPA is a knowledgebase that contains approximately 2,500,000 biological and chemical interactions and functional

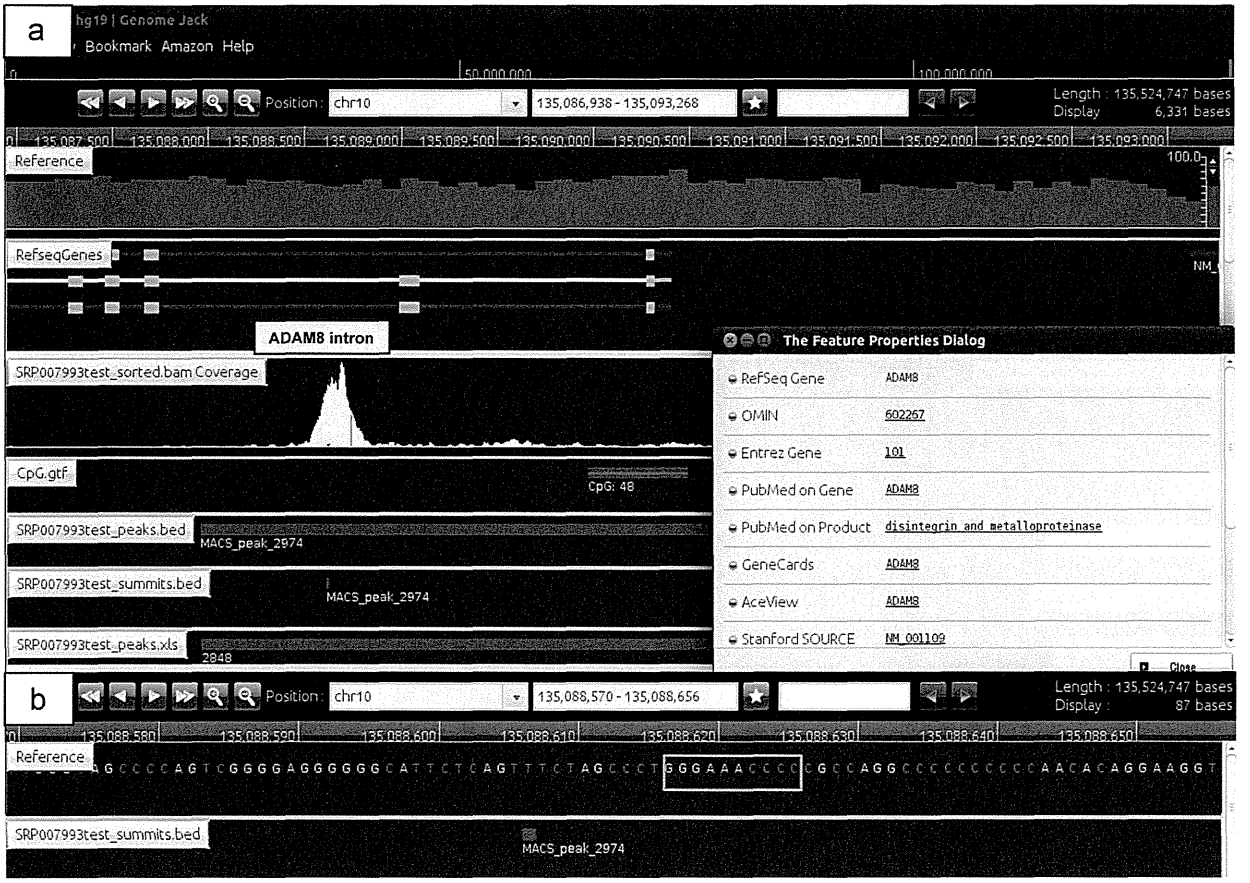


**Fig. 2** Location of NF-κB p65 ChIP-Seq peaks in the intronic region of target genes. The genomic location of the peaks was determined by GenomeJack. An example of ADAM metallopeptidase domain 8 (ADAM8) (Entrez Gene ID 101 in Table 1), composed of three transcript variants NM_001109, NM_001164489, and NM_001164490, is shown, where a MACS peak numbered 2974 is located in the intronic region of ADAM8 (panel a) with a NF-κB consensus sequence motif highlighted by an orange square (panel b). (For interpretation of the references to color in this figure legend, the reader is referred to the web version of this article.)

annotations with definite scientific evidence. By uploading the list of Gene IDs and expression values, the network-generation algorithm identifies focused genes integrated in a global molecular network. IPA calculates the score *p*-value that reflects the statistical significance of association between the genes and the networks by the Fisher's exact test.

KeyMolnet contains knowledge-based contents on 150,500 relationships among human genes and proteins, small molecules, diseases, pathways and drugs (Satoh, 2010). They are categorized into the core contents collected from selected review articles with the highest reliability or the secondary contents extracted from abstracts of PubMed and Human Reference Protein database (HPRD). By importing the list of Gene ID and expression values, KeyMolnet automatically provides corresponding molecules as nodes on the network. The neighboring network-search algorithm selected one or more molecules as starting points to generate the network of all kinds of molecular interactions around starting molecules, including direct activation/inactivation, transcriptional activation/repression, and the complex formation within one path from starting points. The generated network was compared side by side with 484 human canonical pathways of the KeyMolnet library. The algorithm counting the number of overlapping molecular relations between the extracted network and the canonical pathway makes it possible to identify the canonical pathway showing the most significant contribution to the extracted network.

## 4. Results

### 4.1. Identification of 918 ChIP-Seq-based NF-κB p65 target genes

After mapping short reads on hg19, we identified totally 1630 stringent ChIP-Seq peaks that satisfied the criteria of both FDR $\leq$ 0.1% and fold enrichment $\geq$ 10. The genomic location of the peaks was determined by GenomeJack (Figs. 1-3, panel (a). After omitting the peaks located in non-coding genes ($n$=114), those in intergenic regions ($n$=502), and several redundant genes, we extracted 918 peaks located in protein-coding genes. They are tentatively designated as the set of ChIP-Seq-based NF-κB p65 target genes (Supplementary Table 1). They included many genes important for regulation of innate and adaptive immune response and inflammation, such as CD22, CD69, CD70, CD83, CD86, CD209, IL1RN, IL2RG, IL3RA, IL7, IL18R1, IL21R, IL27RA, IL31RA, TGFB1, CXCR4, CX3CL1, TAP1,

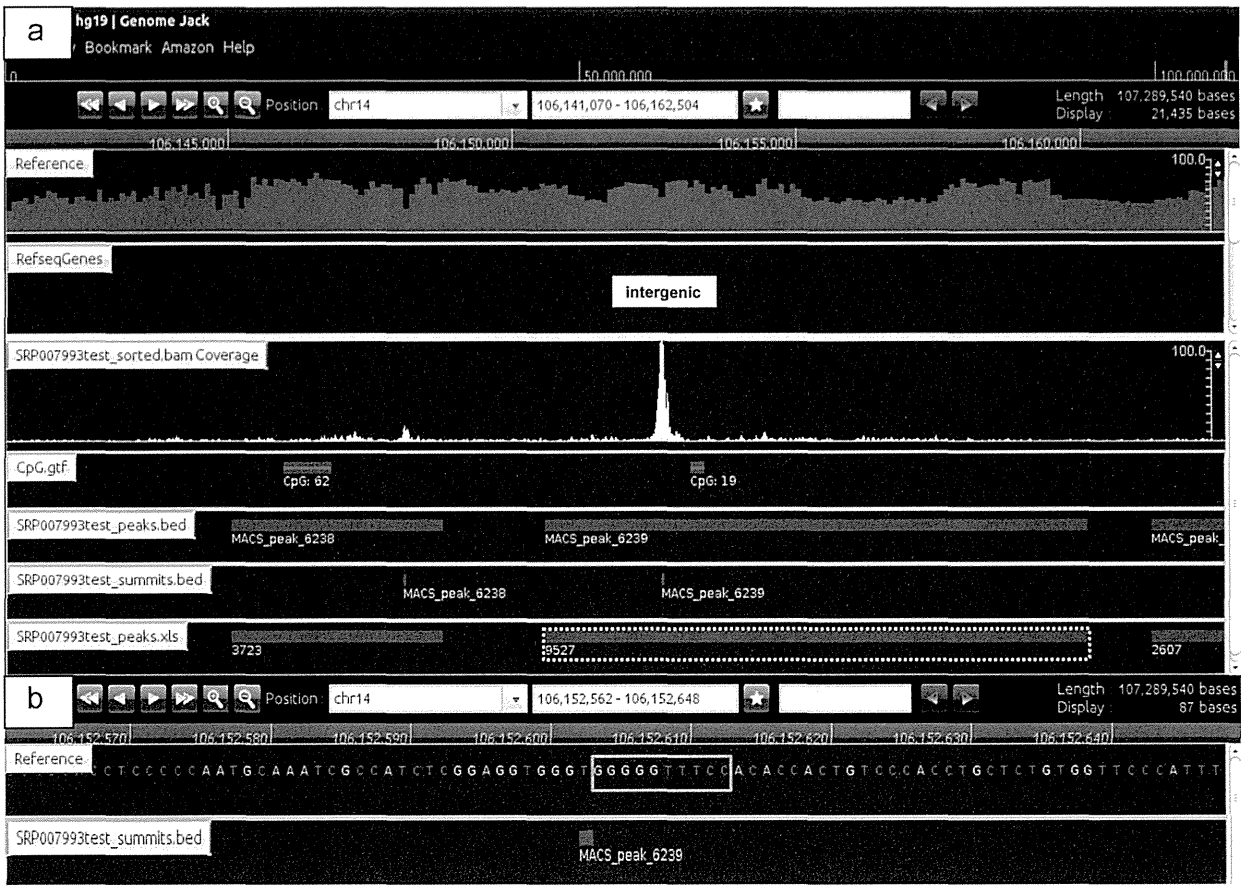


**Fig. 3** Location of NF-κB p65 ChIP-Seq peaks in the intergenic region. The genomic location of the peaks was determined by GenomeJack. An example of intergenic location of a MACS peak numbered 6239 is shown (panel a) with a NF-κB consensus sequence motif highlighted by an orange square (panel b). (For interpretation of the references to color in this figure legend, the reader is referred to the web version of this article.)

**Table 1** Top 30 ChIP-Seq-based NF-κB p65 target genes in human lymphoblastoid cells.

| Chromosome | Start | End | FE | FDR (%) | Location | Gene ID | Gene symbol | Gene name |
|---|---|---|---|---|---|---|---|---|
| chr10 | 135087960 | 135090808 | 51.95 | 0 | Intron | 101 | ADAM8 | ADAM metallopeptidase domain 8 |
| chr21 | 45376690 | 45379750 | 50.41 | 0 | Intron | 56894 | AGPAT3 | 1-acylglycerol-3-phosphate O-acyltransferase 3 |
| chr4 | 86477139 | 86479329 | 44.42 | 0 | Intron | 83478 | ARHGAP24 | Rho GTPase activating protein 24 |
| chr6 | 138186536 | 138200020 | 39.23 | 0 | Promoter | 7128 | **TNFAIP3** | Tumor necrosis factor, alpha-induced protein 3 |
| chr19 | 10496255 | 10498250 | 37.53 | 0 | Promoter | 7297 | TYK2 | Tyrosine kinase 2 |
| chr12 | 111866233 | 111869690 | 37.44 | 0 | Intron | 10019 | SH2B3 | SH2B adapter protein 3 |
| chr4 | 103421036 | 103426349 | 36.81 | 0 | Promoter | 4790 | **NFKB1** | Nuclear factor of kappa light polypeptide gene enhancer in B-cells 1 |
| chr12 | 121997680 | 121999150 | 35.14 | 0 | Intron | 84678 | KDM2B | Lysine (K)-specific demethylase 2B |
| chr1 | 75196627 | 75200204 | 34.45 | 0 | Intron | 1429 | CRYZ | Crystallin, zeta (quinone reductase) |
| chr1 | 75196627 | 75200204 | 34.45 | 0 | Promoter | 127253 | TYW3 | tRNA-yW synthesizing protein 3 homolog (*S. cerevisiae*) |
| chr19 | 36389424 | 36392142 | 34.36 | 0 | Promoter | 10870 | HCST | Hematopoietic cell signal transducer |
| chr19 | 36389424 | 36392142 | 34.36 | 0 | Intron | 84807 | NFKBID | Nuclear factor of kappa light polypeptide gene enhancer in B-cells inhibitor, delta |
| chr16 | 10914391 | 10916414 | 33.92 | 0 | Promoter | 780776 | FAM18A | Family with sequence similarity 18, member A |
| chr7 | 155607589 | 155608757 | 32.79 | 0 | Promoter | 6469 | SHH | Sonic hedgehog homolog (*Drosophila*) |
| chr1 | 37938865 | 37946222 | 32.09 | 0 | Intron | 80149 | ZC3H12A | Zinc finger CCCH-type containing 12A |
| chr17 | 75429437 | 75430665 | 32.06 | 0 | Intron | 10801 | SEPT9 | Septin 9 |
| chr5 | 150456868 | 150463839 | 31.6 | 0 | 5′UTR | 10318 | **TNIP1** | TNFAIP3 interacting protein 1 |
| chrY | 1396361 | 1397638 | 31.44 | 0 | Promoter | 3563 | IL3RA | Interleukin 3 receptor, alpha (low affinity) |
| chr17 | 1376790 | 1378860 | 31.19 | 0 | Exon | 4641 | MYO1C | Myosin IC |
| chr16 | 3012819 | 3014867 | 30.98 | 0 | Promoter | 79412 | KREMEN2 | Kringle containing transmembrane protein 2 |
| chr16 | 3012819 | 3014867 | 30.98 | 0 | Promoter | 124222 | PAQR4 | Progestin and adipoQ receptor family member IV |
| chr22 | 50448174 | 50450362 | 30.14 | 0 | Intron | 400935 | IL17REL | Interleukin 17 receptor E-like |
| chr19 | 45503851 | 45505730 | 30 | 0 | Promoter | 5971 | **RELB** | v-rel reticuloendotheliosis viral oncogene homolog B |
| chr3 | 52344355 | 52345830 | 29.9 | 0 | Promoter | 25981 | DNAH1 | Dynein, axonemal, heavy chain 1 |
| chr10 | 104153066 | 104156567 | 29.62 | 0 | Promoter | 4791 | **NFKB2** | Nuclear factor of kappa light polypeptide gene enhancer in B-cells 2 (p49/p100) |
| chr17 | 61772029 | 61780506 | 29.54 | 0 | Intron | 80774 | LIMD2 | LIM domain containing 2 |
| chr14 | 35868073 | 35876918 | 29.08 | 0 | Promoter | 4792 | **NFKBIA** | Nuclear factor of kappa light polypeptide gene enhancer in B-cells inhibitor, alpha |
| chr9 | 140130602 | 140131876 | 28.81 | 0 | Promoter | 10383 | TUBB4B | Tubulin, beta 2C |
| chr15 | 31803605 | 31804982 | 27.48 | 0 | Intron | 161725 | OTUD7A | OTU domain containing 7A |
| chr7 | 44787088 | 44791813 | 27.47 | 0 | Intron | 83637 | ZMIZ2 | Zinc finger, MIZ-type containing 2 |

From the NF-κB p65 ChIP-Seq dataset numbered SRP007993, we identified 918 stringent peaks on protein-coding genes exhibiting false discovery rate (FDR) ≤0.1% and fold enrichment (FE) ≥10. Top 30 genes based on FE are listed with the chromosome, the position (start, end), FE, FDR, the location (promoter, 5′UTR, exon, intron, 3′UTR), Entrez gene ID, gene symbol, and gene name. Known NF-κB target genes by database search are in bold. The complete list of 918 genes is shown in Supplementary Table 1.

TYK2, IRAK2, NOD2, IRF1, IRF5, STAT1, GATA3, SMAD3, ICAM1, ITGAM, MMP9, FAS, BCL2, and TP53, in addition to NF-κB signaling molecules such as TRAF1, TRAF2, TRAF3, IKBKE, IKBKG, NFKB1, NFKB2, NFKBIA, NFKBIB, NFKBID, NFKBIE, REL, RELA, and RELB. The top 30 genes are listed in Table 1. By searching NF-κB target gene databases, the set of 918 genes included 52 known targets (5.7%), such as ICAM1, IL1RN, IRF1, IRF2, CSF1, NFKBIA, NFKB1, NFKB2, RELB, TNFAIP3, MMP9, TP53, BCK2, and BCL3. The summits of the peaks were located in the promoter ($n$=326; 35.5%), 5′UTR ($n$=49; 5.3%), exon ($n$=23; 2.5%), intron ($n$=504; 54.9%), or 3′UTR ($n$=16; 1.7%) regions. Because we did not study NF-κB p65 ChIP-Seq data of TNFα-unstimulated cells, the possibility could not be excluded that a subset of ChIP-Seq peaks we identified are attributable to the constitutive binding of NF-κB p65 on target genes in the absence of TNFα stimulation.

By motif analysis with MEME-ChIP, both promoter and intronic regions of target genes contained the NF-κB consensus sequence motif, defined as 5′GGG(A/G)N(A/T)(C/T)

(C/T)CC3′ where N accepts any nucleotide (Gilmore, 2006) (Fig. 4, panels a and b), being consistent with the results of GenomeJack (Figs. 1 and 2, panel b). These results validated the specificity of mapping of NF-κB p65 ChIP-Seq short reads onto genomic regions containing the NF-κB consensus sequence motif.

### 4.2. Molecular network of ChIP-Seq-based NF-κB p65 target genes

Next, we studied the molecular network of 918 ChIP-Seq-based NF-κB p65 target genes by using four distinct pathway analysis tools operating on different computational algorithms. DAVID identified functionally associated gene ontology (GO) terms. They include "intracellular signaling cascade" (GO:0007242; $p$=0.0000008), "protein kinase cascade" (GO: 0007243; $p$=0.000004), and "positive regulation of biosynthetic process" (GO:0009891; $p$=0.00003) as the top three3 most significant GO terms (Supplementary Table 2). These results suggest that ChIP-Seq-based NFκB p65 target genes play a role in a wide range of biological functions. KEGG showed close relationships with the "Neurotrophin signaling pathway" (hsa04722; $p$=0.0000004), "B cell receptor signaling pathway" (hsa04662; $p$=0.00008) (Fig. 5), "Small cell lung cancer" (hsa05222; $p$=0.00009), "Apoptosis" (hsa04210; $p$=0.00016), "Pathways in cancer" (hsa05200; $p$=0.0007), "Leukocyte transendothelial migration" (hsa04670; $p$=0.0039), "Prostate cancer" (hsa05215; $p$=0.0042), "Pancreatic cancer" (hsa05212; $p$=0.0054), "Toll-like receptor signaling pathway" (hsa04620; $p$=0.0058), and "Focal adhesion" (hsa04510; $p$=0.0193) (Table 2). Thus, ChIP-Seq-based NF-κB p65 target genes play a pivotal role in regulation of not only immune functions but also oncogenesis. PANTER indicated a significant relationship with the "Apoptosis signaling pathway" (P00006; $p$=0.00321), "B cell activation" (P00010; $p$=0.00326), "Toll receptor signaling pathway" (P00054; $p$=0.0058), "T-cell activation" (P00053; $p$=0.0104), and "Inflammation mediated by chemokine and cytokine signaling pathway" (P00031; $p$=0.0378) (Supplementary Table 3). The core analysis tool of IPA extracted "CD40 signaling" ($p$=4.59E-15), "Molecular Mechanisms of Cancer" ($p$=8.38E-13), and "B Cell Receptor Signaling" ($p$=5.93E-12) as top 3 most significant canonical pathways associated with the set of 918 genes. All of these results support a predominant role of ChIP-Seq-based NF-κB p65 target genes in immune regulation and oncogenesis. Furthermore, IPA extracted the networks defined by "Gene Expression, Developmental Disorder, Hereditary Disorder" ($p$=1.00E-77), "Cellular Function and Maintenance, Cellular Growth and Proliferation, Hematological System Development and Function" ($p$=1.00E-64), and "Cellular Function and Maintenance, Immunological Disease, Cell Signaling" ($p$=1.00E-57) (Fig. 6) as the top three most significant functional networks (Supplementary Table 4).

KeyMolnet by the neighboring network-search algorithm operating on the core contents extracted the highly complex molecular network composed of 3177 molecules and 5489 molecular relations. The network showed the most significant relationship with canonical pathways termed as "transcriptional regulation by p53" ($p$=2.00E-292), "transcriptional regulation by CREB" ($p$=1.44E-238), and "transcriptional regulation by NF-κB" ($p$=1.50E-169) (Supplementary Fig. 1). These results suggest an involvement of the complex cross talk among core transcription factors p53, CREB, and NF-κB in the molecular network of 918 ChIP-Seq-based NF-κB p65 target genes.

### 4.3. ChIP-Seq-based NF-κB p65 target genes corresponding to MS risk alleles and MS lesion-specific proteins

Finally, we studied the relevance of ChIP-Seq-based NFκB p65 target genes to the immunopathogenesis of MS. The recent large-scale collaborative genome-wide association study (GWAS) involving 9772 cases of European origin discovered the collection of 102 MS risk SNPs outside the MHC region (International Multiple Sclerosis Genetics Consortium et al., 2011). They validated 98 of the 102 SNPs overrepresented in MS patients versus the controls. Among the set of 98 genes, we found that CLEC16A, CD86, RGS14, ARHGEF3, TCF7, BATEF, EVI5, RNF213, ODF3B, and ZFP36L1 correspond to ChIP-Seq-based NF-κB p65 target genes.

A different study by a high-throughput proteomics technique comprehensively characterized the profile of MS lesion-specific proteome (Han et al., 2008). They isolated proteins by laser-captured microdissection (LCM) from frozen brain samples of histologically validated acute plaques (AP), chronic active plaques (CAP), or chronic plaques (CP) of progressive MS. Peptide fragments were processed for mass spectrometric analysis. They identified 154, 405 and 231 MS lesion-specific proteins detected exclusively in AP, CAP and CP, respectively. The CAP proteome showed significant relationship with integrin-extracellular matrix interaction (Satoh et al., 2009). We compared 709 MS lesion-specific proteins with 918 ChIP-Seq-based NF-κB p65 target genes. Totally, 49 MS lesion-specific proteins (6.2%) were classified into ChIP-Seq-based NF-κB p65 target genes (Table 3). These results suggest that aberrant regulation of NF-κB-mediated gene expression, by inducing dysfunction of diverse immune functions, is actively involved in development of inflammatory demyelination in MS.

## 5. Discussion

In the present study, we identified 918 NF-κB p65 ChIP-Seq peaks on protein-coding genes from the dataset of TNFα-stimulated human B lymphoblastoid cells. They were located mainly in promoter and intronic regions of target genes with an existence of the NF-κB consensus sequence motif. Our observations are supported by a previous ChIP-Chip study showing that a substantial number of NF-κB-binding sites are located in intronic regions (Martone et al., 2003). Unexpectedly, only 52 genes (5.7%) were known targets by database search, suggesting that both binding of NF-κB and recruitment of appropriate coactivators to responsive elements are crucial for the full-brown activation of target genes (Ziesché et al., 2013). We studied the molecular network of 918 ChIP-Seq-based NF-κB p65 target genes by using four different pathway analysis tools of bioinformatics. KEGG, PANTHER, and IPA consistently showed that the molecular network has significant relationship with regulation of immune functions

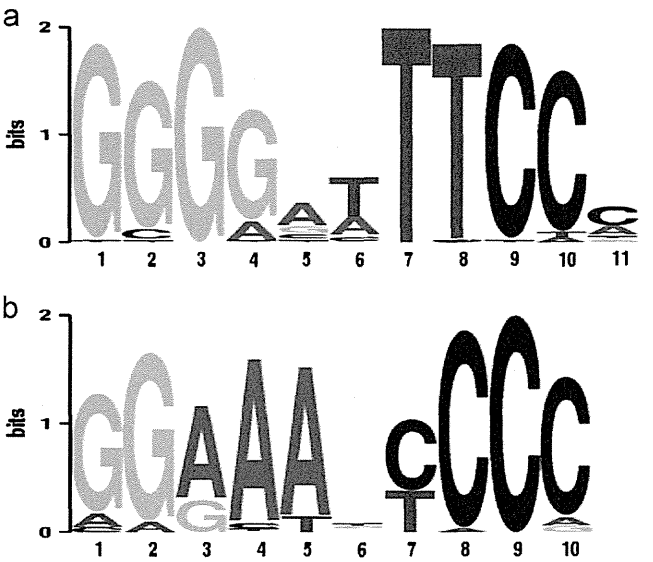


**Fig. 4** Identification of NF-κB consensus sequence motif located in promoter and intronic regions. The consensus sequence motif was identified by importing a 400 bp-length sequence surrounding the summit of MACS peaks of top 50 genes into the MEME-ChIP program, which identified a series of NF-κB consensus sequence motifs as top five most significant motifs in promoter regions (a) and intronic regions (b), typically defined as 5′GGG(A/G)N(A/T)(C/T)(C/T)CC3′, where N accepts any nucleotide.

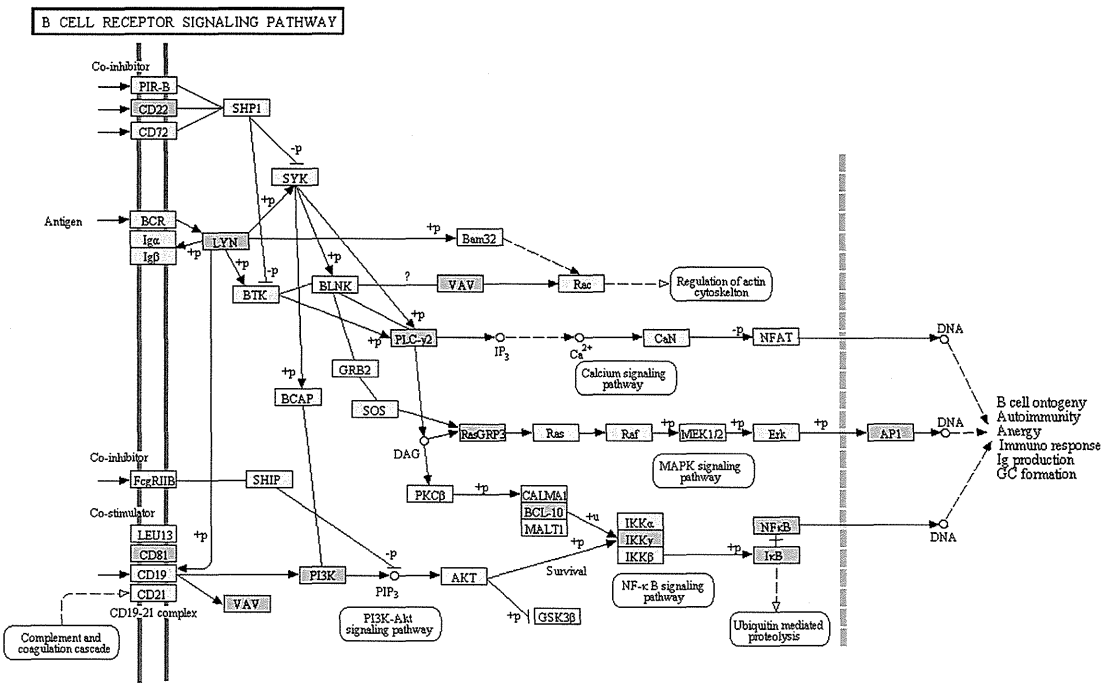


**Fig. 5** KEGG pathways of ChIP-Seq-based NF-κB p65 target genes. Entrez Gene IDs of 918 ChIP-Seq-based NF-κB p65 target genes were imported into DAVID. It identified KEGG pathways relevant to the set of imported genes (Table 2). The second rank pathway termed "B cell receptor signaling pathway" (hsa04662) is shown, where NF-κB p65 target genes is colored orange. (For interpretation of the references to color in this figure legend, the reader is referred to the web version of this article.)

and oncogenesis, including B cell receptor signaling, T cell activation pathway, Toll-like receptor signaling, apoptosis signaling, and molecular mechanisms of cancers. We identified CD22, a negative regulator of B cell receptor signaling (Collins et al., 2006) and CD81, a component of the CD19 complex pivotal for antibody production (van Zelm et al., 2010), as two key genes of ChIP-Seq-based NF-κB p65 targets (Fig. 5). Importantly, recent evidence indicated that B cells play a central role in MS pathogenesis (Krumbholz et al., 2012). However, the possibility could not be excluded that these results are derived from a bias caused by the use of EBV-transformed human B lymphoblastoid cells stimulated

**Table 2** Top 10 KEGG pathways relevant to 918 ChIP-Seq-based NF-κB p65 genes.

| Rank | Category | Genes in the pathway | *p*-Value | FDR | FE |
|---|---|---|---|---|---|
| 1 | hsa04722:Neurotrophin signaling pathway | BCL2, BRAF, CALM1, CAMK4, CSK, FRS2, IRAK2, JUN, MAP3K5, NFKB1, NFKBIA, NFKBIB, NFKBIE, NTRK1, NTRK2, PIK3CA, PIK3CB, PIK3CD, PIK3R1, PLCG2, PRKCD, RAPGEF1, RELA, SH2B2, SH2B3, TP53, TP73 | 0.0000004 | 0.0000036 | 3.858 |
| 2 | hsa04662:B cell receptor signaling pathway | BCL10, CD22, CD81, IKBKG, JUN, LYN, NFKB1, NFKBIA, NFKBIB, NFKBIE, PIK3CA, PIK3CB, PIK3CD, PIK3R1, PLCG2, RASGRP3, RELA, VAV2 | 0.00008 | 0.00064 | 4.252 |
| 3 | hsa05222:Small cell lung cancer | BCL2, BIRC3, CDK6, COL4A2, IKBKG, LAMC2, NFKB1, NFKBIA, PIK3CA, PIK3CB, PIK3CD, PIK3R1, RELA, RXRA, TP53, TRAF1, TRAF2, TRAF3, TRAF4 | 0.00009 | 0.00072 | 4.008 |
| 4 | hsa04210:Apoptosis | BCL2, BIRC3, CAPN2, FAS, IKBKG, IL3RA, IRAK2, NFKB1, NFKBIA, NTRK1, PIK3CA, PIK3CB, PIK3CD, PIK3R1, PRKAR1B, RELA, TNFRSF10B, TP53, TRAF2 | 0.00016 | 0.0013 | 3.869 |
| 5 | hsa05200:Pathways in cancer | BCL2, BIRC3, BRAF, CCDC6, CDK6, COL4A2, CREBBP, CTNNB1, EGF, FAS, FGF2, IKBKG, JUN, KIT, LAMC2, MMP9, NFKB1, NFKB2, NFKBIA, NTRK1, PIK3CA, PIK3CB, PIK3CD, PIK3R1, PLCG2, RALGDS, RARA, RELA, RXRA, SHH, SMAD3, STAT1, TCF7, TGFB1, TP53, TRAF1, TRAF2, TRAF3, TRAF4, WNT10A | 0.0007 | 0.0053 | 2.161 |
| 6 | hsa04670:Leukocyte transendothelial migration | ACTB, ACTG1, BCAR1, CLDN14, CTNNB1, CXCR4, GNAI2, ICAM1, ITGAM, ITK, MMP9, MYL2, MYL5, PIK3CA, PIK3CB, PIK3CD, PIK3R1, PLCG2, VAV2, VCL | 0.0039 | 0.0304 | 3.003 |
| 7 | hsa05215:Prostate cancer | BCL2, BRAF, CREB1, CREBBP, CTNNB1, EGF, IKBKG, NFKB1, NFKBIA, PDGFD, PIK3CA, PIK3CB, PIK3CD, PIK3R1, RELA, TCF7, TP53 | 0.0042 | 0.0333 | 3.384 |
| 8 | hsa05212:Pancreatic cancer | BRAF, CDK6, EGF, IKBKG, NFKB1, PIK3CA, PIK3CB, PIK3CD, PIK3R1, RALGDS, RELA, SMAD3, STAT1, TGFB1, TP53 | 0.0054 | 0.0429 | 3.691 |
| 9 | hsa04620:Toll-like receptor signaling pathway | CD86, IKBKE, IKBKG, IRF5, JUN, MAP2K3, MAP3K8, NFKB1, NFKBIA, PIK3CA, PIK3CB, PIK3CD, PIK3R1, RELA, STAT1, TICAM1, TICAM2, TRAF3 | 0.0058 | 0.0455 | 3.158 |
| 10 | hsa04510:Focal adhesion | ACTB, ACTG1, BCAR1, BCL2, BIRC3, BRAF, CAPN2, COL1A1, COL4A2, CTNNB1, EGF, JUN, LAMC2, MYL2, MYL5, PARVB, PDGFD, PIK3CA, PIK3CB, PIK3CD, PIK3R1, RAPGEF1, SRC, TNR, VAV2, VCL | 0.0193 | 0.1516 | 2.292 |

By importing Entrez gene IDs of 918 ChIP-Seq-based NF-κB p65 target genes into the Functional Annotation tool of DAVID, KEGG pathways showing significant relevance to the imported genes were identified. They are listed with *p*-value corrected by Bonferroni's multiple comparison test, false discovery rate (FDR), and fold enrichment (FE).

with TNFα. It is worthy to note that the epidemiological association of EBV with a risk for development of MS is well established (Levin et al., 2010). We also identified TRAF4, a negative regulator of IL-17 signaling (Zepp et al., 2012) as one of ChIP-Seq-based NF-κB p65 target genes (Fig. 6). KeyMolnet revealed an involvement of the complex crosstalk among core transcription factors, such as NF-κB, p53, and CREB in the NF-κB p65 target gene network, supporting previous observations (Park et al., 2005; Schneider et al., 2010; Oeckinghaus et al., 2011).

Although ChIP-Seq serves as a highly efficient method for genome-wide profiling of DNA-binding proteins, it requires several technical considerations (Landt et al., 2012). The specificity of the antibody, reproducibility of the results, sequencing depth, and the source of controls, along with cell types, developmental stages, and culture conditions capable of affecting epigenetic features, constitute critical factors. In general, DNA-binding of transcription factors is a highly dynamic process. However, the ChIP-Seq data reflect a snapshot of binding actions. Motif analysis of a defined set of high-quality peaks makes it possible to evaluate the antibody specificity to some extent (Landt et al., 2012).

Increasing evidence suggests a central role of aberrant NF-κB activation in the immunopathogenesis of MS. Pathologically, RelA (p65), c-Rel, and p50 subunits of NF-κB are overexpressed in macrophages in active demyelinating lesions of MS (Gveric et al., 1998). RelA (p65) is activated in oligodendrocytes surviving in the lesion edge (Bonetti et al., 1999). Genetically, a predisposing allele in the NFKBIL gene is associated with development of RRMS, while a protective allele in the promoter of the NFKBIA (IκBα) gene is found in the patients with primary progressive MS, suggesting that the NF-κB cascade contributes certainly to susceptibility to MS (Miterski et al., 2002). Targeted disruption of the NFKB1 (p105) gene confers resistance to development of experimental autoimmune encephalomyelitis (EAE), an animal model of MS (Hilliard et al., 1999). In vivo administration of selective inhibitors of NF-κB protects mice from EAE (Pahan and Schmid, 2000). Furthermore, the CNS-restricted inactivation of NF-κB ameliorates EAE, accompanied by suppression of activation of proinflammatory genes in astrocytes (van Loo et al., 2006). We found that 10 genes among 98 MS risk alleles (10.2%) and 49 proteins among 709 MS lesion-specific proteins (6.2%) have met with ChIP-Seq-based

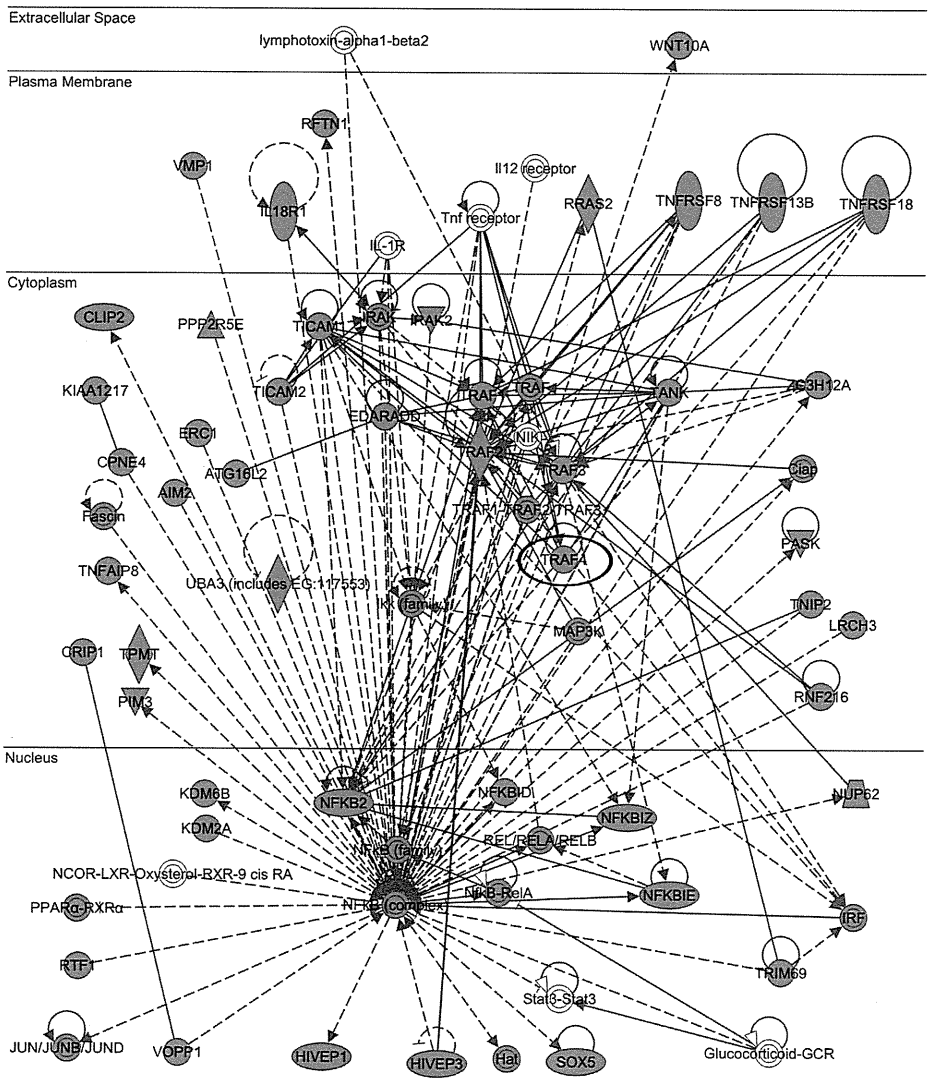


**Fig. 6** IPA functional networks of ChIP-Seq-based NF-κB p65 target genes. Entrez Gene IDs of 918 ChIP-Seq-based NF-κB p65 target genes were imported into the core analysis tool of IPA. It extracted functional networks relevant to the set of imported genes (Supplementary Table 4). The third rank network termed "Cellular Function and Maintenance, Immunological Disease, Cell Signaling" is shown, where NF-κB p65 target genes is colored by red. TRAF4 is highlighted by a blue ellipse. (For interpretation of the references to color in this figure legend, the reader is referred to the web version of this article.)

NF-κB p65 target genes, although it is difficult to evaluate the statistical significance of enrichment of MS-associated genes.

NF-κB acts as a central regulator of various cellular processes (Barnes and Karin, 1997; Pahl, 1999). Actually, molecular network of ChIP-Seq-based NF-κB p65 target genes not only involves immune responses relevant to MS and other autoimmune diseases, such as rheumatoid arthritis (RA) (Myouzen et al., 2012) and systemic lupus erythematosus (SLE) (Zhang et al., 2012), but also regulates oncogenic processes of various cancers. Therefore, we consider that the involvement of molecular network of NF-κB p65 target genes in immune regulation is not a MS-specific phenomenon. However, our results would suggest that deregulation of NF-κB might be actively involved in development and progression of MS, and that drug development targeted to fine-tuning of NF-κB function in autoreactive T and B cells and CNS resident cells could provide a promising approach to suppress the clinical activity of MS (Yan and Greer, 2008).

## 6. Conclusion

We identified the comprehensive set of 918 stringent NF-κB p65 binding sites on protein-coding genes from the ChIP-Seq dataset of TNFα-stimulated human B lymphoblastoid cells. They were located mainly in promoter and intronic regions with an existence of the NF-κB consensus sequence motif. Pathway analysis by KEGG, PANTHER, IPA, and KeyMolnet showed that the NF-κB p65 target gene network is closely associated with the network involved in regulation of diverse immune functions relevant to the immunopathogenesis of MS.

**Table 3** ChIP-Seq-based NF-κB p65 target genes corresponding to MS lesion-specific proteome.

| MS plaque type (p65 targets/ proteome) | Entrez gene ID | Gene symbol | Gene name | UniProt ID |
|---|---|---|---|---|
| AP (10/154) | 375790 | AGRN | Agrin | O00468 |
| | 23092 | ARHGAP26 | Rho GTPase activating protein 26 | Q9UNA1 |
| | 527 | ATP6V0C | ATPase, H+ transporting, lysosomal 16kDa, V0 subunit c | P27449 |
| | 284001 | CCDC57 | Coiled-coil domain containing 57 | Q2TAC2 |
| | 1209 | CLPTM1 | Cleft lip and palate associated transmembrane protein 1 | O96005 |
| | 59269 | HIVEP3 | Human immunodeficiency virus type I enhancer binding protein 3 | Q9BZS0 |
| | 114783 | LMTK3 | Lemur tyrosine kinase 3 | Q96Q04 |
| | 4649 | MYO9A | Myosin IXA | Q9UNJ2 |
| | 5529 | PPP2R5E | Protein phosphatase 2, regulatory subunit B′, epsilon isoform | Q16537 |
| | 54434 | SSH1 | Slingshot homolog 1 (*Drosophila*) | Q8WYL5 |
| CAP (21/405) | 3732 | CD82 | CD82 molecule | P27701 |
| | 1277 | COL1A1 | Collagen, type I, alpha 1 | P02452 |
| | 953 | ENTPD1 | Ectonucleoside triphosphate diphosphohydrolase 1 | P49961 |
| | 54932 | EXD3 | Exonuclease 3′-5′ domain containing 3 | Q8N9H8 |
| | 83856 | FSD1L | Fibronectin type III and SPRY domain containing 1-like | Q9BXM9 |
| | 2902 | GRIN1 | Glutamate receptor, ionotropic, N-methyl D-aspartate 1 | Q05586 |
| | 4151 | MB | Myoglobin | P02144 |
| | 4241 | MFI2 | Antigen p97 (melanoma associated) identified by monoclonal antibodies 133.2 and 96.5 | P08582 |
| | 4641 | MYO1C | Myosin IC | O00159 |
| | 100128731 | OST4 | Oligosaccharyltransferase 4 homolog (*S. cerevisiae*) | P0C6T2 |
| | 55690 | PACS1 | Phosphofurin acidic cluster sorting protein 1 | Q6VY07 |
| | 5142 | PDE4B | Phosphodiesterase 4B, cAMP-specific (phosphodiesterase E4 dunce homolog, *Drosophila*) | Q07343 |
| | 5581 | PRKCE | Protein kinase C, epsilon | Q02156 |
| | 10801 | SEPT9 | Septin 9 | Q9UHD8 |
| | 9644 | SH3PXD2A | SH3 and PX domains 2A | Q5TCZ1 |
| | 6714 | SRC | v-src sarcoma (Schmidt-Ruppin A-2) viral oncogene homolog (avian) | P12931 |
| | 10809 | STARD10 | StAR-related lipid transfer (START) domain containing 10 | Q9Y365 |
| | 6772 | STAT1 | Signal transducer and activator of transcription 1, 91kDa | P42224 |
| | 9144 | SYNGR2 | Synaptogyrin 2 | O43760 |
| | 5976 | UPF1 | UPF1 regulator of nonsense transcripts homolog (yeast) | Q92900 |
| | 152485 | ZNF827 | Zinc finger protein 827 | Q17R98 |
| CP (18/231) | 83478 | ARHGAP24 | Rho GTPase activating protein 24 | Q8N264 |
| | 521 | ATP5I | ATP synthase, $H^+$ transporting, mitochondrial F0 complex, subunit E | P56385 |
| | 8030 | CCDC6 | Coiled-coil domain containing 6 | Q16204 |
| | 1284 | COL4A2 | Collagen, type IV, alpha 2 | P08572 |
| | 51700 | CYB5R2 | Cytochrome b5 reductase 2 | Q6BCY4 |
| | 9732 | DOCK4 | Dedicator of cytokinesis 4 | Q8N1I0 |
| | 26088 | GGA1 | Golgi associated, gamma adaptin ear containing, ARF binding protein 1 | Q9UJY5 |
| | 2788 | GNG7 | Guanine nucleotide binding protein (G protein), gamma 7 | O60262 |
| | 4650 | MYO9B | Myosin IXB | Q13459 |
| | 9612 | NCOR2 | Nuclear receptor co-repressor 2 | Q9Y618 |
| | 23178 | PASK | PAS domain containing serine/threonine kinase | Q96RG2 |
| | 221692 | PHACTR1 | Phosphatase and actin regulator 1 | Q9C0D0 |
| | 5290 | PIK3CA | Phosphoinositide-3-kinase, catalytic, alpha polypeptide | P42336 |
| | 84687 | PPP1R9B | Protein phosphatase 1, regulatory (inhibitor) subunit 9B | Q96B17 |
| | 6146 | RPL22 | Ribosomal protein L22 | P35268 |
| | 6160 | RPL31 | Ribosomal protein L31 | P62899 |

Table 3 (*continued*)

| MS plaque type (p65 targets/ proteome) | Entrez gene ID | Gene symbol | Gene name | UniProt ID |
|---|---|---|---|---|
| | 10044 | SH2D3C | SH2 domain containing 3C | Q8N5H7 |
| | 8027 | STAM | Signal transducing adaptor molecule (SH3 domain and ITAM motif) 1 | Q92783 |

We identified a set of 918 ChIP-Seq-based NF-κB p65 target genes (Suplementary Table 1). We compared these with 790 MS lesion-specific proteins identified by a high-throughput protemics technique (Han et al., 2008). Overlapping genes between both are listed with Entrez Gene ID, gene symbol, gene name, and UniProt ID.

## Conflict of interest

The authors declare no conflict of interest.

## Acknowledgments

This work was supported by grants from the Research on Intractable Diseases (Grant nos. H21-Nanchi-Ippan-201 and H22-Nanchi-Ippan-136), the Ministry of Health, Labour and Welfare (MHLW), Japan, and the High-Tech Research Center (HRC) Project (Grant no. S0801043), the Genome Research Center (GRC) Project, and the Grant-in-Aid (Grant nos. C22500322 and C25430054), the Ministry of Education, Culture, Sports, Science and Technology (MEXT), Japan.

## Appendix A. Supporting information

Supplementary data associated with this article can be found in the online version at http://dx.doi.org/10.1016/j.msard.2013.04.005.

## References

Achiron A, Feldman A, Mandel M, Gurevich M. Impaired expression of peripheral blood apoptotic-related gene transcripts in acute multiple sclerosis relapse. Annals of the New York Academy of Sciences 2007;1107:155-67.

Barnes PJ, Karin M. Nuclear factor-κB. A pivotal transcription factor in chronic inflammatory diseases. New England Journal of Medicine 1997;336:1066-71.

Bonetti B, Stegagno C, Cannella B, Rizzuto N, Moretto G, Raine CS. Activation of NF-κB and c-jun transcription factors in multiple sclerosis lesions. Implications for oligodendrocyte pathology. American Journal of Pathology 1999;155:1433-8.

Brüstle A, Brenner D, Knobbe CB, et al. The NF-κB regulator MALT1 determines the encephalitogenic potential of Th17 cells. Journal of Clinical Investigation 2012;122:4698-709.

Collins BE, Smith BA, Bengtson P, Paulson JC. Ablation of CD22 in ligand-deficient mice restores B cell receptor signaling. Nature Immunology 2006;7:199-206.

Comabella M, Khoury SJ. Immunopathogenesis of multiple sclerosis. Clinical Immunology 2012;142:2-8.

Eggert M, Goertsches R, Seeck U, Dilk S, Neeck G, Zettl UK. Changes in the activation level of NF-kappa B in lymphocytes of MS patients during glucocorticoid pulse therapy. Journal of the Neurological Sciences 2008;264:145-50.

Gerstein MB, Kundaje A, Hariharan M, et al. Architecture of the human regulatory network derived from ENCODE data. Nature 2012;489:91-100.

Gilmore TD. Introduction to NF-κB: players, pathways, perspectives. Oncogene 2006;25:6680-4.

Gregersen PK, Amos CI, Lee AT, et al. *REL*, encoding a member of the NF-κB family of transcription factors, is a newly defined risk locus for rheumatoid arthritis. Nature Genetics 2009;41:820-3.

Gveric D, Kaltschmidt C, Cuzner ML, Newcombe J. Transcription factor NF-κB and inhibitor IκBα are localized in macrophages in active multiple sclerosis lesions. Journal of Neuropathology and Experimental Neurology 1998;57:168-78.

Han MH, Hwang SI, Roy DB, et al. Proteomic analysis of active multiple sclerosis lesions reveals therapeutic targets. Nature 2008;451:1076-81.

Hayden MS, West AP, Ghosh S. NF-κB and the immune response. Oncogene 2006;25:6758-80.

Hilliard B, Samoilova EB, Liu TS, Rostami A, Chen Y. Experimental autoimmune encephalomyelitis in NF-κB-deficient mice: roles of NF-κB in the activation and differentiation of autoreactive T cells. Journal of Immunology 1999;163:2937-43.

Huang da W, Sherman BT, Lempicki RA. Systematic and integrative analysis of large gene lists using DAVID bioinformatics resources. Nature Protocols 2009;4:44-57.

International Multiple Sclerosis Genetics Consortium, Wellcome Trust Case Control Consortium 2, Sawcer S, et al. Genetic risk and a primary role for cell-mediated immune mechanisms in multiple sclerosis. Nature 2011;476:214-9.

Kasowski M, Grubert F, Heffelfinger C, et al. Variation in transcription factor binding among humans. Science 2010;328:232-5.

Krumbholz M, Derfuss T, Hohlfeld R, Meinl E. B cells and antibodies in multiple sclerosis pathogenesis and therapy. Nature Reviews Neurology 2012;8:613-23.

Landt SG, Marinov GK, Kundaje A, et al. ChIP-Seq guidelines and practices of the ENCODE and modENCODE consortia. Genome Research 2012;22:1813-31.

Levin LI, Munger KL, O'Reilly EJ, Falk KI, Ascherio A. Primary infection with the Epstein-Barr virus and risk of multiple sclerosis. Annals of Neurology 2010;67:824-30.

Lindsey JW, Agarwal SK, Tan FK. Gene expression changes in multiple sclerosis relapse suggest activation of T and non-T cells. Molecular Medicine 2011;17:95-102.

Martone R, Euskirchen G, Bertone P, et al. Distribution of NF-κB-binding sites across human chromosome 22. Proceedings of the National Academy of Sciences of the United States of America 2003;100:12247-52.

Martín-Saavedra FM, Flores N, Dorado B, et al. Beta-interferon unbalances the peripheral T cell proinflammatory response in experimental autoimmune encephalomyelitis. Molecular Immunology 2007;44:3597-607.

Miterski B, Böhringer S, Klein W, et al. Inhibitors in the NFκB cascade comprise prime candidate genes predisposing to

multiple sclerosis, especially in selected combinations. Genes and Immunity 2002;3:211-9.
Myouzen K, Kochi Y, Okada Y, et al. Functional variants in NFKBIE and RTKN2 involved in activation of the NF-κB pathway are associated with rheumatoid arthritis in Japanese. PLoS Genetics 2012;8:e1002949.
Oeckinghaus A, Hayden MS, Ghosh S. Crosstalk in NF-κB signaling pathways. Nature Immunology 2011;12:695-708.
Pahan K, Schmid M. Activation of nuclear factor-κB in the spinal cord of experimental allergic encephalomyelitis. Neuroscience Letters 2000;287:17-20.
Pahl HL. Activators and target genes of Rel/NF-κB transcription factors. Oncogene 1999;18:6853-66.
Park JM, Greten FR, Wong A, et al. Signaling pathways and genes that inhibit pathogen-induced macrophage apoptosis. CREB and NF-κB as key regulators. Immunity 2005;23:319-29.
Park PJ. ChIP-Seq: advantages and challenges of a maturing technology. Nature Reviews Genetics 2009;10:669-80.
Rothwarf DM, Karin M. The NF-κB activation pathway: a paradigm in information transfer from membrane to nucleus. Science's STKE 1999;1999. RE1.
Satoh J, Misawa T, Tabunoki H, Yamamura T. Molecular network analysis of T-cell transcriptome suggests aberrant regulation of gene expression by NF-κB as a biomarker for relapse of multiple sclerosis. Disease Markers 2008;25:27-35.
Satoh J, Tabunoki H. Molecular network of ChIP-Seq-based vitamin D receptor target genes. Multiple Sclerosis; 2013 [in press]. PMID: 23401126. DOI: 10.1177/1352458512471873.
Satoh J. Bioinformatics approach to identifying molecular biomarkers and networks in multiple sclerosis. Clinical and Experimental Neuroimmunology 2010;1:127-40.
Satoh JI, Tabunoki H, Yamamura T. Molecular network of the comprehensive multiple sclerosis brain-lesion proteome. Multiple Sclerosis 2009;15:531-41.
Schneider G, Henrich A, Greiner G, et al. Cross talk between stimulated NF-κB and the tumor suppressor p53. Oncogene 2010;29:2795-806.
Sica A, Dorman L, Viggiano V, et al. Interaction of NF-κB and NFAT with the interferon-γ promoter. Journal of Biological Chemistry 1997;272:30412-20.
Viatour P, Merville MP, Bours V. Chariot A. Phosphorylation of NF-κB and IκB proteins: implications in cancer and inflammation. Trends in Biochemical Sciences 2005;30:43-52.
Yan J, Greer JM. NF-κBa potential therapeutic target for the treatment of multiple sclerosis. CNS & Neurological Disorders: Drug Targets 2008;7:536-57.
van Loo G, De Lorenzi R, Schmidt H, et al. Inhibition of transcription factor NF-κB in the central nervous system ameliorates autoimmune encephalomyelitis in mice. Nature Immunology 2006;7:954-61.
van Zelm MC, Smet J, Adams B, et al. CD81 gene defect in humans disrupts CD19 complex formation and leads to antibody deficiency. Journal of Clinical Investigation 2010;120:1265-74.
Zepp JA, Liu C, Qian W, et al. Cutting edge: TNF receptor-associated factor 4 restricts IL-17-mediated pathology and signaling processes. Journal of Immunology 2012;189:33-7.
Zhang W, Shi Q, Xu X, et al. Aberrant CD40-induced NF-κB activation in human lupus B lymphocytes. PLoS One 2012;7: e41644.
Ziesché E, Kettner-Buhrow D, Weber A, et al. The coactivator role of histone deacetylase 3 in IL-1-signaling involves deacetylation of p65 NF-κB. Nucleic Acids Research; 2013;41:90-109. http://dx.doi.org/10.1093/nar/gks916.

# Efficacy of the anti–IL-6 receptor antibody tocilizumab in neuromyelitis optica

## A pilot study

OPEN

Manabu Araki, MD, PhD
Takako Matsuoka, MD
Katsuichi Miyamoto, MD, PhD
Susumu Kusunoki, MD, PhD
Tomoko Okamoto, MD, PhD
Miho Murata, MD, PhD
Sachiko Miyake, MD, PhD
Toshimasa Aranami, MD, PhD
Takashi Yamamura, MD, PhD

Correspondence to Dr. Yamamura: yamamura@ncnp.go.jp

### ABSTRACT

**Objective:** To evaluate the safety and efficacy of a humanized anti-interleukin-6 receptor antibody, tocilizumab (TCZ), in patients with neuromyelitis optica (NMO).

**Methods:** Seven patients with anti-aquaporin-4 antibody (AQP4-Ab)-positive NMO or NMO spectrum disorders were recruited on the basis of their limited responsiveness to their current treatment. They were given a monthly injection of TCZ (8 mg/kg) with their current therapy for a year. We evaluated the annualized relapse rate, the Expanded Disability Status Scale score, and numerical rating scales for neurogenic pain and fatigue. Serum levels of anti-AQP4-Ab were measured with AQP4-transfected cells.

**Results:** Six females and one male with NMO were enrolled. After a year of TCZ treatment, the annualized relapse rate decreased from 2.9 ± 1.1 to 0.4 ± 0.8 ($p < 0.005$). The Expanded Disability Status Scale score, neuropathic pain, and general fatigue also declined significantly. The ameliorating effects on intractable pain exceeded expectations.

**Conclusion:** Interleukin-6 receptor blockade is a promising therapeutic option for NMO.

**Classification of evidence:** This study provides Class IV evidence that in patients with NMO, TCZ reduces relapse rate, neuropathic pain, and fatigue. *Neurology*® 2014;82:1302-1306

### GLOSSARY

**Ab** = antibody; **AQP4** = aquaporin-4; **AZA** = azathioprine; **EDSS** = Expanded Disability Status Scale; **IL** = interleukin; **IL-6R** = interleukin-6 receptor; **NMO** = neuromyelitis optica; **PB** = plasmablasts; **PSL** = prednisolone; **TCZ** = tocilizumab.

Neuromyelitis optica (NMO) is a relatively rare autoimmune disease that predominantly affects the spinal cord and optic nerve. Anti–aquaporin-4 antibody (AQP4-Ab), which is a disease marker of NMO, has an important role in causing the destruction of astrocytes that express AQP4.[1] Empirically, the use of disease-modifying drugs for multiple sclerosis, including interferon β, is not recommended for NMO,[2] which is consistent with the distinct pathogenesis of NMO and multiple sclerosis. We have recently described that plasmablasts (PB), which are a subpopulation of B cells, increased in the peripheral blood of patients with NMO and that PB are a major source of anti-AQP4-Ab among peripheral blood B cells.[3] In addition, we observed that exogenous interleukin (IL)-6 promotes the survival of PB and their production of anti-AQP4-Ab in vitro. Given the increased levels of IL-6 in the serum and CSF during relapses of NMO,[1,3] we postulated that blocking IL-6 receptor (IL-6R) pathways might reduce the disease activity of NMO by inactivating the effector functions of PB. A humanized anti–IL-6R monoclonal antibody, tocilizumab (TCZ) (Actemra/RoActemra), has been approved in more than 100 countries for use in the treatment of rheumatoid arthritis.[4] Herein, we describe our clinical study that aimed to explore the efficacy of TCZ in NMO.

Editorial, page 1294

From the Multiple Sclerosis Center (M.A., T.O., S.M., T.A., T.Y.) and Department of Neurology (T.O., M.M.), National Center Hospital, and Department of Immunology, National Institute of Neuroscience (T.M., S.M., T.A., T.Y.), National Center of Neurology and Psychiatry, Tokyo; Department of Neurology (K.M., S.K.), Kinki University School of Medicine, Osaka; and Department of Pediatrics (T.M.), Graduate School of Medicine, University of Tokyo, Japan.

Go to Neurology.org for full disclosures. Funding information and disclosures deemed relevant by the authors, if any, are provided at the end of the article.

Table Demographics of the patients

| | Patient | | | | | | |
|---|---|---|---|---|---|---|---|
| | 1 | 2 | 3 | 4 | 5 | 6 | 7 |
| Age, y/sex | 37/F | 38/F | 26/F | 31/M | 55/F | 62/F | 23/F |
| Age at onset, y | 23 | 27 | 21 | 12 | 38 | 60 | 21 |
| Anti-AQP4-Ab | + | + | + | + | + | + | + |
| Myelitis | + | + | + | + | + | + | – |
| Optic neuritis | + | + | + | + | + | + | + |
| EDSS score | 3.5 | 6.5 | 3.5 | 6.0 | 6.5 | 6.5 | 3.0 |
| Total no. of relapses | 20 | 9 | 6 | 16 | 20 | 3 | 7 |
| ARR before TCZ | 3 | 2 | 2 | 2 | 3 | 3 | 5 |
| Immunotherapies for exacerbations | IVMP, PLEX | IVMP, PLEX | IVMP, PLEX | IVMP, OBP, PLEX | IVMP, PLEX | IVMP, PLEX | IVMP, PLEX |
| Past immunotherapies | IFNβ, IVIg | IFNβ | — | IFNβ, MITX | IFNβ, AZA | — | AZA |
| Present immunotherapies | PSL, AZA | AZA | PSL | PSL, AZA | PSL, CyA | PSL, CyA | PSL, tacrolimus |
| Neuropathic pain (e.g., girdle pain), NRS | 4 | 4 | 2 | 4 | 4 | 3 | 0 |
| General fatigue, NRS | 5 | 8 | 6 | 7 | 5 | 3 | 9 |
| Pain and antispasticity medication | GBP, CZP, NTP, NSAID | CZP, mexiletine, NTP, tizanidine, NSAID | — | CBZ, baclofen, NSAID | CBZ | PGB | — |

Abbreviations: AQP4-Ab = aquaporin-4 antibody; ARR = annualized relapse rate; AZA = azathioprine; CBZ = carbamazepine; CZP = clonazepam; CyA = cyclosporine; EDSS = Expanded Disability Status Scale; GBP = gabapentin; IFNβ = interferon β; IVIg = IV immunoglobulin; IVMP = IV methylprednisolone; MITX = mitoxantrone; NRS = numerical rating scale; NSAID = nonsteroidal anti-inflammatory drug; NTP = Neurotropin (an extract from the inflamed skin of vaccinia virus–inoculated rabbits); OBP = oral betamethasone pulse therapy; PGB = pregabalin; PLEX = plasma exchange; PSL = prednisolone; TCZ = tocilizumab.

**METHODS Level of evidence.** The aim of this Class IV evidence study was to evaluate the effect and safety of a monthly injection of TCZ (8 mg/kg) with their current therapy in patients with NMO. We evaluated the adverse events based on Common Terminology Criteria for Adverse Events, version 4.0.

**Standard protocol approvals, registrations, and patient consents.** All patients gave written informed consent before the first treatment with TCZ. The institutional ethical standards committee on human experimentation approved this clinical study. The study is registered with University Hospital Medical Information Network Clinical Trials Registry, numbers UMIN000005889 and UMIN000007866.

**Patients and treatment.** Seven patients who met the diagnostic criteria of NMO in 2006 were enrolled after providing informed consent (table). Results of chest x-rays, interferon γ release assays, and plasma 1,3-β-D-glucan measurement excluded latent tuberculosis and fungal infection. All of the patients had been treated with combinations of oral prednisolone (PSL) and immunosuppressants, including azathioprine (AZA). Nevertheless, they had at least 2 relapses during the year before enrollment (figure 1). Among their past immunomodulatory medications, interferon β had been prescribed in 4 patients before the anti-AQP4-Ab assay became available. Although symptomatic treatments had been provided, the patients experienced general fatigue and intractable pain in their trunk and limbs. There were no abnormalities in their routine laboratory blood tests. Neither pleocytosis nor increased levels of IL-6 were observed in the CSF. MRI revealed high-intensity signals in the optic nerves and longitudinally extensive lesions in the spinal cord. All patients except one had scattered brain lesions. A monthly dose (8 mg/kg) of TCZ was added to the patients' oral corticosteroid and immunosuppressive drug regimen.

**Clinical and laboratory assessment.** As clinical outcome measures, we evaluated alterations in the number of relapses, Expanded Disability Status Scale (EDSS) scores, and pain and fatigue severity scores (numerical rating scales). A relapse was defined as an objective exacerbation in neurologic findings that lasted for longer than 24 hours with an increase in the EDSS score of more than 0.5. Brain and spinal cord MRI scans were examined every 4 or 6 months. CSF examinations, sensory-evoked potentials, and visual-evoked potentials were also evaluated at the time of entry into the study and 12 months later. We measured serum anti-AQP4-Ab levels by evaluating the binding of serum immunoglobulin G to AQP4 transfectants, as previously described.[5] All outcome measures were analyzed with nonparametric Wilcoxon rank-sum tests, with the use of 2-tailed statistical tests at a significance level of 0.05.

**RESULTS** After starting TCZ treatment, the total number of annual relapses in the patients significantly reduced (figures 1 and 2). Notably, 5 of the 7 patients were relapse-free after starting TCZ. The relapses observed in patients 1 and 5 were mild and their symptoms recovered after IV methylprednisolone. On average, the annualized relapse rate reduced from 2.9 ± 1.1 (range, 2–5) during the year before study to 0.4 ± 0.8 (range, 0–2) during the year after